ANALYSIS OF SINGLE POLE AUTO RECLOSURE IN EXTRA HIGH VOLTAGE SYSTEMS

BY

SAHALA TURNIP

This thesis is submitted as fulfillment of the requirements
for the degree of master of technology
in
Department of Electrical and Electronic Engineering
University of Tasmania
Australia

Supervisor

Dr Marian Piekutowski

June 1995

DECLARATION

To the best of my knowledge, this thesis contains no material previously published or written by another person, except where due reference is made in the text of the thesis.

SAHALA TURNIP

ACKNOWLEDGMENTS

Thank you to my supervisor Dr Marian Piekutowski for his time, assistance and encouragement in the development of this thesis. Without his assistance and permission to use computer facilities in the HEC, this thesis would not have been completed. I also wish thank you to my employer PT. PLN Pusat, for giving me leave to continue this study; and to my sponsor, AUSAID, for providing the scholarship. And also thank you to Mrs Roslyn Stoddart for proof reading.

ABSTRACT

The successful single pole auto reclosure (SPAR) operation in the EHV system increases system stability, improves system reliability, reduces reclosing overvoltages and torsional impacts on generator shafts. The success rate of a SPAR operation is dependent on the time required to extinguish the secondary arc and to rebuild the dielectric strength of the de-ionized arc path. The extinction time of the secondary arc depends on the magnitude of the secondary arc current and the recovery voltage. Without a compensation scheme, a SPAR operation will be unsuccessful in a long EHV transmission line. Based on a three phase reduced system model, the performance of the main parameters of SPAR operations, the secondary arc current and the recovery voltage were analyzed. Detailed sensitivity analysis of SPAR operation in a long single circuit 500 kV transmission line was investigated for different line transposition scheme, line length, prefault line load and fault location using EMTDC software. A review of SPAR compensation methods is also included. Obtained results indicate a strong correlations between conductor configuration, line transposition schemes, line length, prefault line loading, fault location and compensation scheme, and the secondary arc current and the recovery voltage of SPAR operations.

LIST OF SYMBOLS

I_s	=	the total secondary arc current
I_{sc}	=	the secondary arc current due to capacitive coupling
I_{sl}	=	the secondary arc current due to inductive coupling
V_r	=	the recovery voltage
Z_A	=	the line series self impedance of phase A
$Z_{(A,B)}$	=	the line mutual series impedance of phasė A and phase B
$Y_C(i,k)$	=	the line mutual admittance of phase i and phase k
$x_{(i,k)}$	=	the line mutual reactance of phase i and phase k
Y_p	=	the reactor phase admittance
Y_n	=	the reactor neutral admittance
X_p	=	the reactor phase reactance
X_n	=	the reactor neutral reactance
I	=	the healthy phase line current
V	=	the healthy phase voltage
$C_m = C_{(A,B)}$	=	the line shunt mutual capacitance of phase A and phase B
$C_g = C_{(A,g)}$	=	the line shunt capacitance of phase A to ground
C_1	=	the line positive sequence shunt capacitance
C_0	=	the line zero sequence shunt capacitance
F	=	the degree of line positive sequence compensation
B_1	=	the reactor positive sequence inductive susceptance
B_0	=	the reactor zero sequence inductive susceptance
B_n	=	the reactor neutral inductive susceptance
$B_1^{'}$	=	the line positive sequence capacitive susceptance
$B_0^{'}$	=	the line zero sequence capacitive susceptance
$B_n^{'}$	=	the line neutral capactive susceptance
a	=	$Cos120^0 + j\,Sin120^0$

CONTENTS

CHAPTER 1

INTRODUCTION

Planning and constructing a new extra high voltage (EHV) transmission line to expand or to strengthen an existing power system, becomes more difficult for utilities because of increasing economic and environmental pressures. Therefore, there is a strong interest in new technologies and analytical methods to improve power system reliability and to increase power transfer capability of the existing transmission systems. Single-pole auto-reclosing (SPAR) has been used as a cost-effective method to increase system reliability [9]. Some favorable factors to apply SPAR operation in EHV systems are:

- Single line to ground (SLG) is the most frequently (over 90% [10]) occuring faults due to lightning in EHV systems
- most of these faults are transient and rapidly self-clearing [10]
- while the faulty phase is disconnected the remaining two healthy phases of a single circuit line continue to transfer 67% of pre fault power.

Many utilities around the world succesfully apply SPAR in EHV systems. Experiences of the Indonesia State Electricity Company (PLN) indicate that in the period from 1985 to 1992, 93 % of all faults in 500 kV systems were single line to ground faults and that 63 % of SPAR operations were successful. The probability of multi-phase fault in EHV systems is very low due to large spaces between phase conductors.

The successful SPAR operation increases system transient stability, because the synchronizing power of the two systems is still connected through the healthy phases during the interruption period. Successful SPAR operation reduces the

severity of a disturbance, such as reclosing overvoltages and torsional impact on generator shaft, compared to a three phase opening and reclosing circuit breaker. In some cases implementation of SPAR may even delay the requirement for construction of additional transmission lines. A SPAR scheme is suitable for a remote generator station which is connected to load centers through a single or double circuit transmission.

Under SPAR operation only the faulted phase will open to isolate the fault, and following a time delay required to extinguish the secondary arc and to restore the dielectric strength of the arc path, the circuit breakers rapidly reclose. However, immediately after the primary arc is extinguished, a secondary arc will exist in the same arc path as a result of electrostatic (capacitive) and electromagnetic (inductive) coupling between the energized phases and the open phase. This secondary arc must be extinguished before reclosing the circuit breakers. If the secondary arc duration, the time from the last circuit breaker open until the extinction of the secondary arc, is longer than the reclosing dead time, then the SPAR operation will fail, and the relay will open circuit breakers in all three phases. The length of the dead time is based on the system stability requirements.

The successful operation of SPAR depends on many factors including: primary fault current, secondary arc current, recovery voltage across the arc path, length of arc path, fault location, wind velocity, and other factors. From all of those factors, the secondary arc and recovery voltage are the most important and their influence can be reduced by the implementation of compensation schemes. Other factors listed above as influencing SPAR operation cannot be controlled practically.

Over the years, extensive research, field and laboratory experiments have been conducted to develop an effective way to reduce the secondary arc current and the recovery voltage in order to ensure the circuit breakers rapid reclosing without a

reduction of SPAR operation success rates. There are three methods to prevent unsuccessful SPAR operations, namely:

- neutralize the mutual capacitance between the healthy phases and the faulted phase
- discharge the secondary arc current
- natural arc extinction.

A four-legged reactor connected on the line side of a circuit breaker or a capacitance placed parallel with the circuit breaker can be applied to neutralize the mutual capacitance between two healthy phases and the faulted one. The are three basic designs for such reactors:

- a four-legged reactor with equal phase reactances effectively to compensate the mutual coupling of a transposed transmission line [13,14]
- a switched four-legged reactor to compensate the effects of an untransposed transmission line [4,22,23]
- an asymmetrical four-legged reactor, also to compensate for the effects of an untransposed transmission line [21].

The High Speed Grounding Switch (HSGS) method is used to discharge the secondary arc. Immediately after the faulted phase was isolated, both ends open line are earthed to ground through resistors to remove the driving voltage behind the secondary arc [10]. After the extinction of the secondary arc, the switch resistors open first before the circuit breakers reclose [7]. This method is applicable for an uncompensated transmission line.

The natural extinction of secondary arc current is only appropriate for a short length transmission line and when the system stability allow a relatively long dead time.

Objectives

The objective of this thesis is to analyze selected physical and design factors affecting operation of SPAR, and to understand the computer modelling of a transmission system for fast transient study based on SPAR simulation by using EMTDC software. The simulation investigated the sensitivity of the secondary arc current and the recovery voltage of SPAR operation with such factors, namely:

- the effect of line transposition
- the effect of faulted phase
- the effect of shunt reactors
- the effect of prefault load flow
- the effect of fault location.

One objective of this study was to establish an understanding of modelling requirements, in particular modelling of components, system reduction and model verification, for SPAR analysis in EHV system by using a computer program like EMTDC. This type of expertise can be directly applicable to the other electromagnetic transients studies in the EHV system, such as: switching overvoltages caused by line energization or load rejection, lightning surge studies, or insulation coordination studies. An electromagnetic transient study is one of the most difficult studies in power systems analysis [2], and a very important tool to design a 500 kV system. A computer simulation for electromagnetic studies are extremely effective, cheaper and more versatile compared to staged fault tests, laboratory test or Transient Network Analyzer.

CHAPTER 2

METHODS

There are three methods to simulate a SPAR operation:

- laboratory or staged fault test experiment
- Transient Network Analyzer (TNA) and
- Digital Computer Simulation.

It is important to emphasize that all the methods complement each other. There is no one superior method. The staged fault test result is the most accurate, but this method imposes constraints on system operations and it is much more expensive compared to the other methods. The staged fault tests of an existing system are conducted only if the TNA and Digital Computer results do not correspond to operational experience.

The preliminary studies are usually conducted by digital computer. Occasionally, if necessary, the TNA studies are also carried out to calibrate models and to verify digital computer results.

2.1 The staged fault test

To conduct a laboratory or a staged fault test to determine the secondary arc duration, requires enormous resources. Usually a staged fault test is done during the construction periods, before the transmission line is commissioned into commercial service. These tests are usually carried out only for lines connecting power station into a larger system. To replicate a single line to ground fault a special structure is built. The fault is initiated by a small stainless steel wire, one end attached to the ground bus and another end connected to a fiberglass insulating

rod. By using a spring loaded mechanism, the fiberglass starts to contact the conductor with the ground through the stainless steel wire [3,5,12,20,24].

A high fidelity measurement system is needed to monitor the experiment process. High speed digital recorders are used for recording phase to ground fault voltage, reactor neutral voltage, primary fault current, and secondary arc current. One or two high speed cameras, which provide 600 to 1200 color frames per second are used to record the arc current in cycles from the initiation of the fault until the last circuit breaker recloses. Normally, the experiment is carried out over a relatively long period, to investigate the effects of wind velocity on secondary arc extinction.

The staged fault test results represent the real behaviour of SPAR operation. From repetitive SPAR operations under different conditions, one can infer the correlation of the success rate of SPAR operation with the secondary arc current, the recovery voltage, fault location, prefault line loading, wind velocity, weather condition and other environment factors. However the test requires a large amount of resources, in terms of money and out of service time of the line.

2.2 Transient Network Analyzer

The second method uses Transient Network Analyzer (TNA) to simulate the actual power systems behaviour by modelling the appropriate components of the systems in a miniature network consisting of resistor, inductor and capacitor. The transmission line characteristics are modelled with the same ohmic value at the system frequency. Meanwhile, the voltage and current quantities are scaled. For example, 1 Volt in the model is equal to 1000 Volts in the system, and 1 A in the model represents 1 kA in the system. The generators are modelled to include the effects of rotating mass, voltage regulator and prime mover governor, so that they can respond to system changes as in the actual condition [6].

The TNA is energized by a three-phase generator which represents an infinite bus. The characteristics of other sources are represented by their appropriate inductance and capacitance source.

The simulation of a single line to ground fault in TNA is conducted as in the real systems. The circuit breaker, which is modelled by a solid state switch, such as a silicon thyristor controlled rectifier, can be programmed to open after the fault occurs and reclose after extinction of the secondary arc. The secondary arc current and the recovery voltage are monitored through a computer screen. Experience shows that the TNA results agree with the staged fault test results.

The TNA facilities cost is about $ 3,000,000 to $ 10,000,000; but utilities can hire the facilities in the USA, Canada or European countries.

2.3 Digital Computer

The digital computer simulation for power systems transient studies now almost takes over the function of TNA. Most utilities conduct transient studies by using digital computers, because digital computer facilities are easier to access than a laboratory facility such as TNA. Also, the cost of a computer and simulation software (approximately $50,000 to $100,000) is much cheaper than hiring TNA facilities. The other advantage of digital computer simulations is that the results are easy to store, retrieve and replicate various scenarios in a shorter time compared to time required to assemble network model in TNA facilities.

The most popular electrical transient program is the Electromagnetic Transient Program (EMTP) which was originally developed by the Bonneville Power Administration (BPA) in cooperation with many other utilities and universities.

The program computes transient differential equations by using trapezoidal integration methods, starting from the initial conditions specified by the user.

The system to be studied is modelled by nodes linked by branches. Depending on the type of simulation, different models of branches are provided in EMTP.

The EMTP program is distributed by EPRI (Electric Power Research Institute), USA. The data entry process for the system models is tedious, because the input file is in FORTRAN format, sensitive to column location. Every component of the systems has different input format. The operation of EMTP program is not user friendly and requires significant experience. Another software program which emanated from EMTP, called ATP (Alternative Transient Program) was developed by the University in Lueven, Belgium. This software has similar disadvantages as EMTP mainly time consuming data interface. However, this is the only free of charge software.

PSCAD/EMTDC is a commercial software to simulate electromagnetic transients, and was developed by Manitoba, HVDC Research Centre, Canada. This software is equipped with CAD based user interface and therefore it is more user friendly. The process of building an input file in EMTDC program is based on dragging the system component from a diagram library to the work space to assemble the required network configuration. For example, a transmission line section is represented by two transmission towers diagram. A generator data is inputted by copying a generator diagram from the model library to the work space frame.

The EMTDC software has a similar theoretical basis of the solution methods to the EMTP program [16]. The main difference is in the user interface of the program. The program consists of the following modules: T-Line, Cable, Draft, Run-Time, Uniplot and Multiplot. The T-Line and Cable packages are used for calculating

transmission line parameters and cable parameters for user specified transmission conductor geometry, conductor type, conductor configuration, and shielding. For example the input data required for the transmission parameter calculation include the geometrical data of the tower, resistance of conductor and earth wire, and earth resistivity.

The Draft layout module is used to assemble graphically the power system under investigation by using the graphical icons available from the icon library facility. To input an individual component data, choose and drag the appropriate icon of the component onto a drawing canvas (worksheet), then a special menu will appear on the screen to request the data. The buswork icons, representing zero impedance connections, are used to interconnect the individual components.

The transient phenomena is simulated by using timed breaker logic and timed fault logic facilities. For example, to simulate a single line to ground fault, a very low value resistor is connected from a phase to the ground. The SPAR operation is simulated by using a timed fault logic facility to pre-define the fault initiation time and the fault duration. The opening time, the reclosing time and the initial condition data of a circuit breaker is entered by using timed breaker logic facility.

After successfully building and compiling a base case system configuration, further study is carried out by Run-Time module. The running process (computer execution) can be monitored and controlled while it is in progress through plotting diagrams, graphical icon meters or a slider to interactively display various quantities of the power system as they are being calculated.

For reporting purposes, EMTDC software is equipped with the Uniplot and the Multiplot modules. Data produced by Run-Time simulation can be stored and later directly plotted and analyzed using Uniplot module. The Multiplot module

has been provided to combine and display a group of graphs from different study cases on a common page.

The study of behaviour of SPAR operations in this thesis was carried out using EMTDC software program in an IBM RISC System/6000 Work Station Computer of the Hydro Electric Commission, Tasmania.

The following procedure was adopted in this study:

1. the investigated transmission line was defined;
2. the transmission line characteristics, which are dependent on geometry of tower, conductor configuration and type, line shielding, ground conditions etc., was calculated using the T-Line module;
3. the reduced three phase system model suitable for analysis of SPAR operation was prepared and compiled the model using the Draft module;
4. the fault and switching sequence for the simulation was defined;
5. the parameters to be monitored during calculation process were defined;
6. the simulation process was carried out using the Run-Time module;
7. the results of simulation was analyzed using the Uniplot or Multiplot module.

To reduce the model of an interconnected system into a transmission line segment suitable for studying SPAR performance, the external equivalent system is used to include effects of the short circuit contribution from parts of the system connected to each line end. The short circuit source is represented as a constant voltage behind the short circuit equivalent reactance. This model is valid since the contributions of the travelling wave from other busbars have no effect on the secondary arc current and the recovery voltage under investigation. Investigated secondary arc current and the recovery voltage are predominantly influenced by the transmission line with a phase isolated by SPAR operation.

CHAPTER 3

OPERATION OF SPAR

If a single line to ground fault occurs, the protective system must be able to distinguish the faulted phase and issue a trip signal to the appropriate breaker poles to isolate the faulted phase. After the short circuit (primary) arc current is extinguished, a secondary arc current exists in the established arc path due to capacitive and inductive coupling between the healthy phases and the faulted phase. Moreover, after the extinction of the secondary arc current and before the circuit breakers are reclosed, there is a recovery voltage induced by the same mutual capacitive and inductive coupling between the energized phases and the open phase. If the recovery voltage is high enough it will cause arc restrike resulting in unsuccessful SPAR operation.

In an EHV transmission line of more than 100 km length, the secondary arc current and the recovery voltage are quite large. Without any compensation scheme, it will take a long time for the secondary arc to self-extinguish. If this time is greater than a dead setting time, line protection will detect a permanent fault and disconnect the line from service, also locking out the SPAR and thus preventing further reclosure.

Before analyzing methods to reduce the secondary arc current, the following are mathematical formulations of the secondary arc current and the recovery voltage.

3.1 Secondary Arc Current

The secondary arc current (I_s) is maintained by the contribution of capacitive (I_{sc}) and inductive (I_{sl}) coupling between the healthy phases and the open phase.

Therefore, the total secondary arc current is equal to the phasor sum of the two currents

$$I_s = I_{sc} + I_{sl} \qquad (3.1.)$$

Secondary arc current due to capacitive coupling

Consider Figure-3.1, a model of transmission line consisting of two buses connected by an equivalent pi-section, which describes the capacitive and the inductive mutual coupling between phases [22]. For the transversal analysis, the longitudinal self-impedance and the resistive losses associated with reactive elements are ignored.

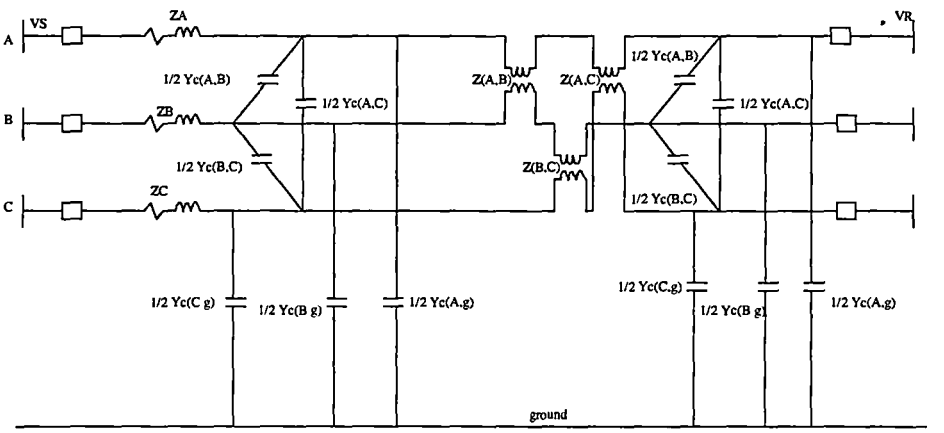

Figure-3.1: The mutual equivalent of a transmission line.

From circuit analysis theory, the secondary arc current due to capacitive coupling in the open phase mainly depends on the line voltage and the interphase admittance, that is:

$$I_{sc}(i) = Y_c(i,k)V(k) + Y_c(i,h)V(h) \qquad (3.2)$$

where: i is the faulted phase,

k, h are the healthy phases,

$$V(k) = \frac{V_R(k) + V_S(k)}{2},$$

V(k) is the average voltage of the healthy phase.

The secondary arc current due to capacitive coupling depends on the healthy phase voltage and the mutual interphase admittance between the faulted phase and the healthy phases, which almost remain constant along the line. It is not dependent on the fault location or the prefault load. Therefore, the secondary arc current due to capacitive coupling is relatively constant along the line.

For a fault in phase B (middle phase), then :

$$\begin{aligned} I_{sc}(B) &= Y_c(A,B)V(A) + Y_c(B,C)V(C) \\ &= [Y_c(A,B) + aY_c(B,C)]V(A) \end{aligned} \qquad (3.3)$$

If fault in phase A (outer phase), then :

$$\begin{aligned} I_{sc}(A) &= Y_c(A,B)V(B) + Y_c(A,C)V(C) \\ &= [Y_c(A,B) + a^2Y_c(A,C)]V(B) \end{aligned} \qquad (3.4)$$

For an untransposed line, the mutual admittance between outer-middle phase is much higher (3 to 4 times) than the mutual admittance between outer-outer phase (phase A-C). Therefore the magnitude of $I_{sc}(B)$ for the middle phase is much higher than $I_{sc}(C)$ or $I_{sc}(A)$ (outer phases), and the magnitude of secondary arc current due to capacitive coupling for the outer phases are equal.

On the other hand, for a transposed line, the diagonal elements of admittance matrix have approximately the same value, and the off-diagonal elements or the mutual admittances also have equal values (Appendix-1). Therefore, the secondary arc current in the disconnected phase due to the capacitive coupling is the same for any phase of a transposed line. The following section illustrates the

calculation of the secondary arc current due to capacitive coupling of a transposed line.

Suppose a SLG fault occurs on phase B of an ideally transposed line. The phase to ground capacitance of each phase is C_0 and the interphase mutual capacitance is $\frac{1}{3}(C_1 - C_0)$ (Appendix-1). By transforming the mutual capacitance from delta to star connection and considering that phase voltages are balanced, the transversal representation of the single line diagram for a SLG in phase B and both CBs open on the faulted phase is shown in Figure-3.2.

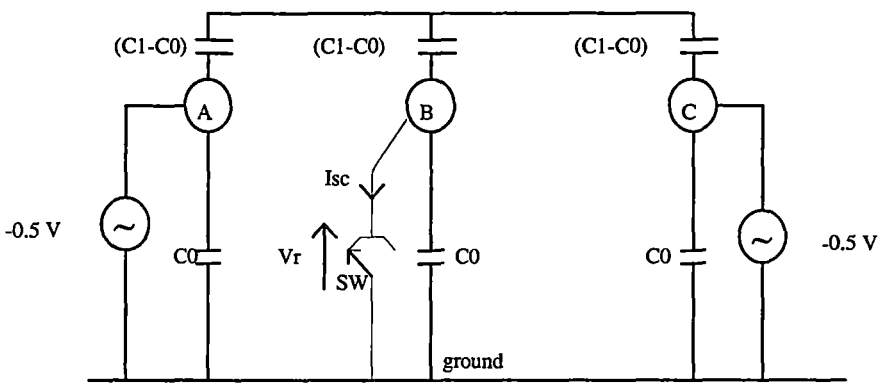

Figure-3.2: Star connection of capacitive coupling of SLG fault on an ideally transposed line.

Since the phase voltages are balanced, $V(C) = a^2V(B)$ and $V(A) = aV(B)$ then the magnitude of the real part of phase C and phase A are equal, $V(A) = V(C) = -0.5V(B)$. Meanwhile the imaginary parts have the same magnitude but the opposite sign, so their contributions cancel each other in the open phase. The Thevenin diagram of Figure-3.2 can be simplified by folding phase A on phase C as shown in Figure-3.3.

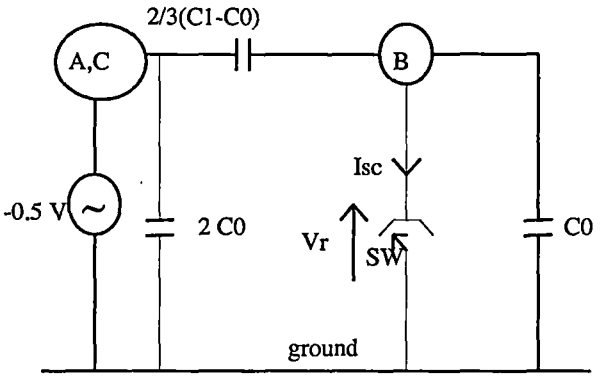

Figure-3.3: The Thevenin diagram of Figure-3.2.

From circuit diagram on Figure-3.3 the secondary arc current due to capacitive coupling can be stated as:

$$I_{sc} = -\frac{V}{3} j(B_1' - B_0') \qquad \text{(A/km)} \qquad (3.5)$$

Where $B = \omega C$ (mho/km) is the distributed capacitive susceptance of the line,

V is the healthy phase voltage.

Secondary arc current due to inductive coupling

According to electromagnetic theory, the load currents in the healthy phases produce an electromagnetic field surrounding the conductor and induce a voltage to the conductor inside the field. Therefore the inductive component of the secondary arc current I_{sl} depends on the load current in the healthy phases, the mutual reactance of each phase, and the phase to ground admittance of the open phase $Y_c(i,g)$.

$$I_{sl}(i) = -Y_c(i,g)[x_{(i,h)} I_h + x_{(i,k)} I_k] \qquad (3.6)$$

The contribution of the interphase inductive coupling to the secondary arc current is variable and it depends on the fault location and the prefault load current.

The electromagnetic coupling diagram of a transposed line when a SLG fault occurs in the end of the line can be shown in Figure-3.4 [10].

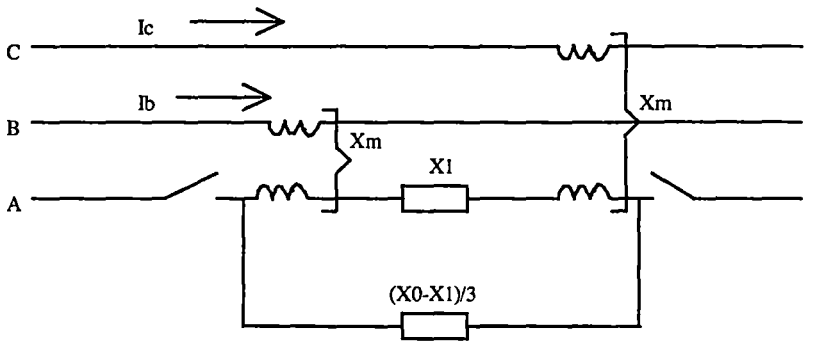

Figure-3.4: Electromagnetic coupling diagram

Then, the secondary arc current due to mutual inductive coupling for a SLG fault in the end of the line is as follows

$$I_{sl} = \frac{(I_B + I_C)X_m}{\frac{1}{3}(X_1 + X_2 + X_0)} \qquad (3.7)$$

On the other hand, if a SLG fault occurs in the midpoint of the line, the secondary arc current due to mutual inductive coupling is zero, because the current from each end is circulating and thus cancels each other [10].

3.2 Recovery Voltage

The recovery voltage is built up across the arc path immediately after the secondary arc extinction and before the circuit breakers reclose by the same interphase mutual coupling sources as the secondary arc current.

Since the contribution of the inductive interphase coupling is dependent on the fault location and the prefault loading condition, the following formula of the recovery voltage considers only the contribution from the capacitive coupling.

In delta connection of mutual interphase capacitance, the transversal diagram of a SLG fault on phase B of Figure-3.2 is shown in Figure-3.5. And the Thevenin diagram of Figure-3.5 is displayed in Figure-3.6.

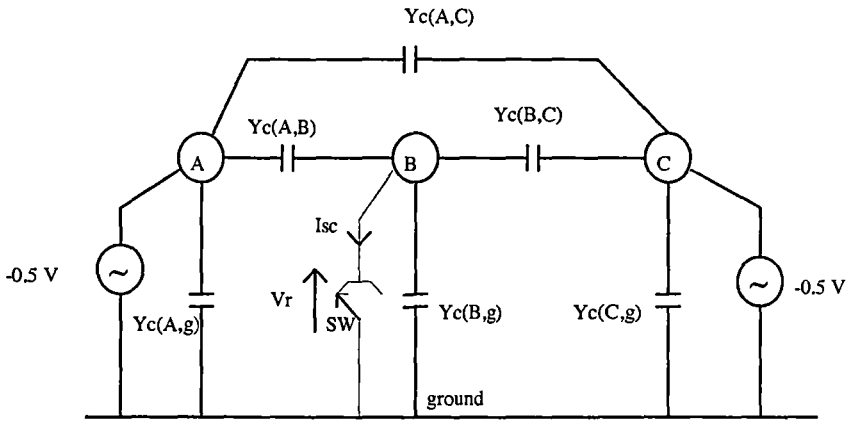

Figure-3.5: Delta connection of electrostatic coupling with the faulted phase open.

The recovery voltage on phase B after fault clearing, denoted by opening switch SW in Figure-3.6, is :

$$V_r = -0.5V \frac{\dfrac{1}{j\omega C_{(B,g)}}}{\dfrac{1}{j\omega[C_{(A,B)} + C_{(B,C)}]} + \dfrac{1}{j\omega C_{(B,g)}}} = -0.5V \frac{C_{(A,B)} + C_{(B,C)}}{C_{(A,B)} + C_{(B,C)} + C_{(B,g)}} \tag{3.8}$$

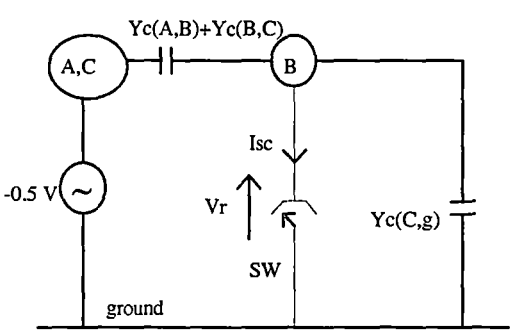

Figure-3:6: The Thevenin equivalent of electrostatic coupling.

It is clear from (3.8) that for an untransposed transmission line, the recovery voltage of the middle phase is higher than the outer phase. However, for an ideally

transposed transmission line the recovery voltage is the same for a single line to ground fault in any phase. By examining Figure-3.3, the recovery voltage for a transposed line is:

$$V_r = V\frac{(C_1 - C_0)}{(C_0 + 2C_1)} \qquad (3.9)$$

If the recovery voltage is high, it will cause the secondary arc restrike, which will prevent a successful SPAR operation.

3.3 Secondary Arc Duration

Based on laboratory and staged fault test experiments, it can be stated that the secondary arc extinction duration has a strong correlation with the secondary arc current and the recovery voltage. Under normal condition an air path behaves as an ideal gas and a pure dielectric. When a SLG-fault occurs, the primary current will cause a very high temperature in the air path. This high temperature creates free electrons and ions in the gas. The free electrons generated by the heating can transfer an electric current as in a metal. When the primary arc current is interrupted, the thermal hysterisis of the path will allow the smaller secondary arc current to flow until the cooling process extinguishes the secondary arc current. Due to ionization and residue of the conducting plasma, after the secondary arc current extinction, the air path dielectric strength is weakened. If the recovery voltage is greater than the air path dielectric strength, a dielectric reignition will occur [12]. Therefore, the smaller the secondary arc current and the recovery voltage are, the faster the arc extinction would be.

In practical design, the secondary arc duration is expected not to exceed 0.5 sec if the secondary arc current and the recovery voltage are limited to about 20 A rms and 50 kV respectively [3,11]. Figure-A2.1 (Appendix-2) displays laboratory

results of secondary arc duration as a function of the secondary arc current and the recovery voltage for the 1000 kV transmission lines [21]. Figure-A2.2 (Appendix-2) shows the relationship between the secondary arc current and the gradient recovery voltage for transmission line with operating voltage up to 700 kV [8,17].

CHAPTER 4

METHODS FOR REDUCING THE SECONDARY ARC CURRENT

The function of an EHV transmission line is to transfer bulk power from remote generator stations to load centres, or between interconnected systems or load centres. Formulae presented in the previous chapter indicate that the magnitude of the secondary arc current and the recovery voltage in a long EHV transmission line are large. The high voltage level and the length of transmission line contribute a high secondary arc current due to interphase capacitive coupling, and load current increases the secondary arc current due to interphase inductive coupling. Without any compensation scheme, the arc extinction duration of a SLG fault in a EHV line with length of more than 100 km is normally significantly longer than the dead time allowed by the system stability. To ensure a successful SPAR operation, many types of compensation schemes have been implemented and tested. This chapter presents an overview of most common compensation schemes for limiting the secondary arc current and the recovery voltage.

4.1 Capacitor across Circuit Breaker

The method was proposed in 1969 [19]. To explain the nullifying mutual capacitance proposed in this method, assume the analysed transmission line is fully transposed. Hence, the mutual capacitance (C_m) of each phase has a common value and the capacitance to ground (C_g) of each phase is equal. By transforming the mutual capacitance into a star connection, the condition of open CB to isolated a SLG fault in phase A can be shown in Figure-4.1 [19].

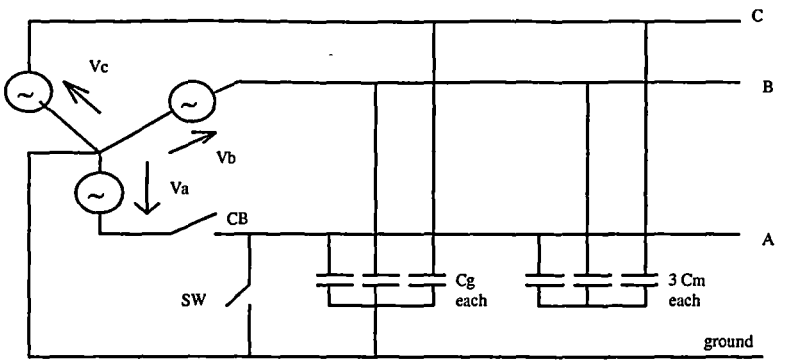

Figure-4.1: Lumped capacitance of three-phase system.

The Thevenin equivalent of a circuit presented above is shown in Figure-4.2.

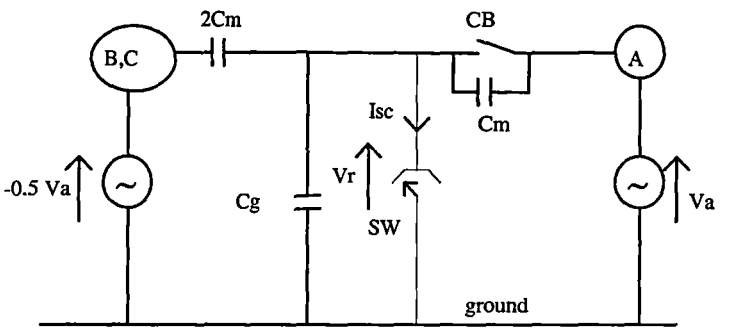

Figure-4.2: The Thevenin diagram of fault in phase A.

Without a capacitor across the open circuit breaker the secondary arc current I_{sc} is:

$$I_{sc} = -V_a j\omega C_m \qquad (4.1)$$

If a capacitor C_m is installed across the open circuit breaker Figure-4.2, then the source voltage V_a will induce a current through the fault with the same magnitude but in the opposite direction to I_{sc}. Therefore, the total secondary arc current becomes zero, and the recovery voltages V_r across SW also becomes zero.

Theoretically, this method has been proven almost as effective as the four-legged reactor scheme. However, from an economic point of view this scheme is more expensive compared to the four-legged scheme, since most of long EHV

transmission lines are already equipped with shunt reactors for reactive compensation and voltage control purpose.

4.2 High-Speed Grounding Switch (HSGS)

The grounding method to extinguish secondary arc current was first suggested in 1948 [18]. The procedural operation of HSGS scheme is as follows: after a SLG fault occurs, the CB at both ends of the faulted phase open to clear the primary fault. Then the HSGS at each end close, grounding the faulted phase and reducing the secondary arc. Finally, the HSGS at each end should open first before both the CB are reclosed [7]. The diagram of the HSGS connection is shown in Figure-4.3.

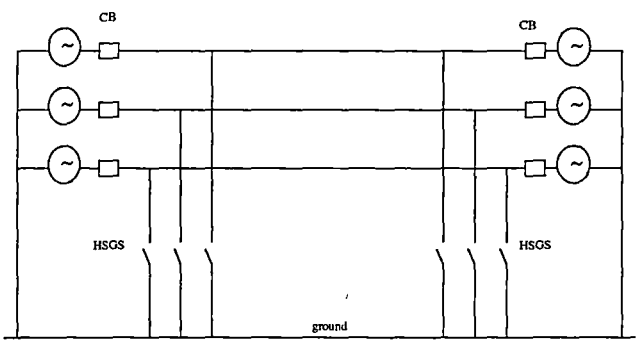

Figure-4.3: The diagram of the HSGS connection to each phase.

By closing the HSGS at both ends of the faulted phase, two closed loops are formed through the earth, each loop consisting of the HSGS and the secondary arc. The currents in the two sound phases induce a voltage in the two loops, hence creating currents i_1 and i_2 that are superimposed on the arc current (Figure-4.4). Since the instantaneous values of i_1 and i_2 are in the opposite direction, the total secondary arc current will decrease. The grounding of the faulty phase also causes the recovery voltage induced by the two healthy phases to decrease, ensuring the successful extinction of the secondary arc [7,10].

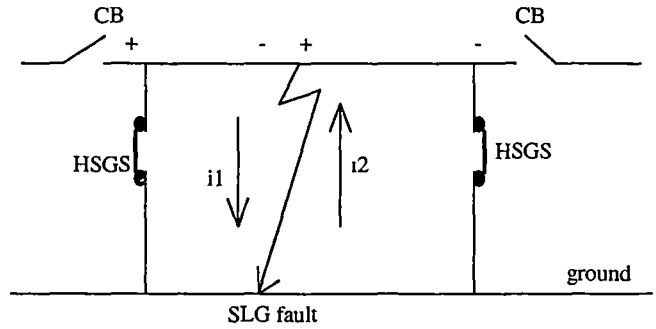

Figure-4.4: The instantaneous currents due to induced voltage from energized phases.

The staged fault test for HSGS was conducted in 1979 on the 196 km long, 500 kV transmission line by Bonneville Power Administration, USA. The result shows that the secondary arc current was extinguished immediately after HSGS closed [7].

The successful test results convinced BPA to apply HSGS for SPAR on the lines which may not require shunt reactors for the reactive power compensation purpose [7,18]. In other cases application of the four-legged reactor is prefered.

4.3 Four-Legged reactor

Long EHV transmission lines require installation of shunt reactor to compensate the reactive power line charging at light load condition, and to limit the switching overvoltages during line energization or under load rejection. By using an appropriate connection, the same reactor bank can be utilized to improve the extinction of the secondary arc current during SPAR operations. A neutral reactor is connected between the neutral point of the star reactor bank and the ground to compensate the interphase capacitive coupling [14]. Only a fractional increase in cost is needed for the neutral reactor, because the insulation level and the thermal capacity of the neutral reactor is lower than the phase reactors. This scheme effectively compensates the interphase capacitve coupling but has less effect on the inductive coupling. To fully compensate both capacitive and inductive interphase coupling, a 100 % phase compensation factor is required. This is not practical

since it would result in high, potential damaging voltage resonance and also it will further depress voltage level under heavy load conditions [15].

The way in which the four-legged reactors suppress the secondary arc current can be analyzed by recalling the relationship between voltages and currents for the capacitance admittance matrix as follows:

$$\begin{bmatrix} I_a \\ I_b \\ I_c \end{bmatrix} = \begin{bmatrix} Y_{aa} & Y_{ab} & Y_{ac} \\ Y_{ab} & Y_{bb} & Y_{bc} \\ Y_{ac} & Y_{bc} & Y_{cc} \end{bmatrix} \begin{bmatrix} V_a \\ V_b \\ V_c \end{bmatrix} \qquad (4.2)$$

When a SLG fault occurs in phase A, the secondary arc current is fed through the capacitive coupling between phases, which is represented by the off-diagonal elements of the admittance matrix in equation (4.2). By installing a four-legged reactor (Figure-4.5) with suitably selected inductances in the transmission line, the off-diagonal matrix elements will be eliminated, hence reducing the secondary arc current.

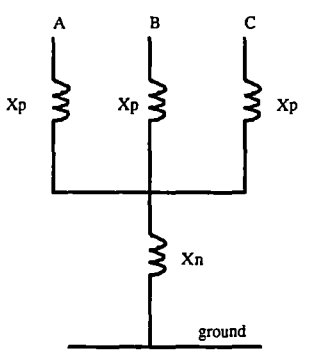

Figure-4.5: The symmetrical four-legged reactor connection.

The admittance matrix of a four-legged reactor is as follow :

$$\frac{1}{3Y_p + Y_n} \begin{bmatrix} Y_p(2Y_p + Y_n) & -Y_p^2 & -Y_p^2 \\ -Y_p^2 & Y_p(2Y_p + Y_n) & -Y_p^2 \\ -Y_p^2 & -Y_p^2 & Y_p(2Y_p + Y_n) \end{bmatrix} \qquad (4.3)$$

By selecting the appropriate value of the neutral reactor, the symmetrical four-legged reactor can effectively compensate the interphase capacitive coupling and ensure succesful SPAR operation of a fully transposed line. The following section describes a procedure to determine the size of the neutral reactor of a transposed line.

The line capacitance diagram in Figure-3.2. can be transformed into a four-legged form as shown in Figure-4.6 [13].

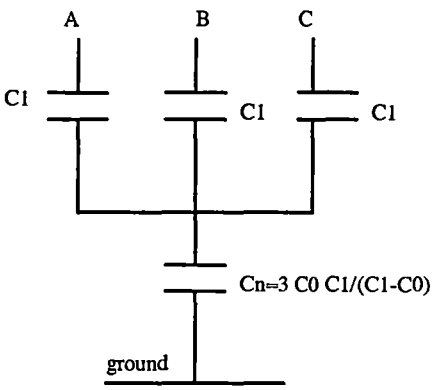

Figure-4.6: Four-legged diagram of line capacitances.

Since the reactors are in parallel with line capacitances, it is more convenient to express their value in terms of susceptance B instead of reactance X. Denote unprimed letters B and X as the inductive susceptance and reactance respectively, and primed letters B' and X' stand for the respective capacitive quantities.

Suppose the line shunt compensation factor is F, therefore

$$F = \frac{B_1}{B_1'} \qquad (4.4)$$

Then the reactors susceptance required to compensate the mutual interphase capacitance is :

$$B_1 - B_0 = B_1' - B_0' \qquad (4.5)$$

Substituting (4.4) to (4.5) then :

$$B_0 = B_0' - (1-F)B_1' \qquad (4.6)$$

By back substitution, the of reactor reactance values are calculated in terms of line susceptances as [13]:

$$X_p = \frac{1}{FB_1'} \qquad (4.7)$$

$$X_n = \frac{1}{FB_n' \left[1-(1-F)\frac{B_1'}{B_0'}\right]} \qquad (4.8)$$

$$\text{where } B_n' = \frac{3B_0'B_1'}{B_1' - B_0'} \qquad (4.9)$$

Therefore the size of the neutral reactor is dependent on the line shunt compensation factor (F) required for the steady state conditions.

However, because of the unequal interphase capacitance of untransposed lines, the conventional symmetrical four-legged reactor is not able to reduce effectively the secondary arc of an untransposed line. The mid-outer mutual capacitance is much higher than the mutual capacitance between the outer phases.

There are two practical designs of the four-legged reactor to compensate the interphase mutual coupling of an untransposed line. The first scheme, is based on the asymmetrical four-legged reactor, where the size of each reactor is determined to match unequal phase admittances of the lines [21]. There are four reactances to be defined from three interphase capacitance equations.

The second scheme is using a combination of a symmetrical four-legged reactor and a switched four legged reactor connection [4,22,23]. The symmetrical four-legged reactor is used to compensate the mutual capacitance between the outer phases, while the additional switched four-legged reactor is used to compensate the mid-outer phase capacitance. The off-diagonal elements of the switched four-

legged reactor admittance matrix will vary depending on the faulted phase. The operation of the switches is coordinated with the line circuit breakers. The switch position for phase-to-ground fault in different phases is shown in Figure-4.6 [4,22,23].

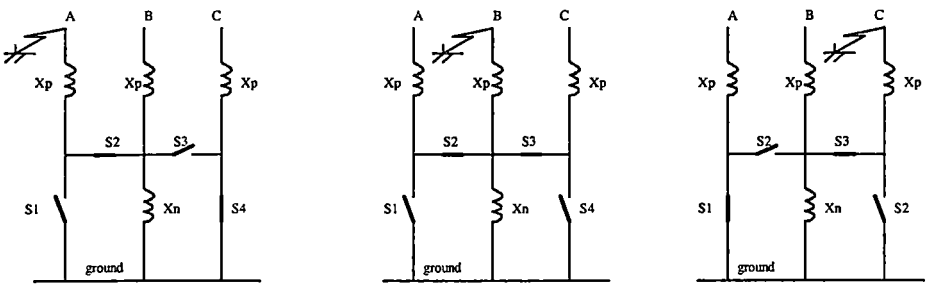

Figure-4.6: Scheme 2, switch positions for phase-to-ground faults in different phases.

Figure-4.6 indicates that the reactor admittance matrix for single-phase-to-ground fault in the middle phase (phase B) is similar to the reactor admittance of the symmetrical reactor.

However, for a SLG fault in phase A (the outer phase), the reactor admittance matrix is as follows:

$$\frac{1}{2Y_p + Y_n}\begin{bmatrix} Y_p(Y_p+Y_n) & -Y_p^2 & 0 \\ -Y_p^2 & Y_p(Y_p+Y_n) & 0 \\ 0 & 0 & Y_p(2Y_p+Y_n) \end{bmatrix} \quad (4.10)$$

In the same way, the reactor admittance for a fault in phase C can be calculated. The value of neutral reactor X_n is optimized to minimize the secondary arc current [22].

CHAPTER 5

SIMULATIONS

5.1 Overview of Java-Bali Power System

The existing PLN Indonesia Java-Bali transmission system consists of 3 voltage levels, namely : 500 kV, 150 kV and 70 kV networks. The 500 kV transmission network has a very essential role in the Java-Bali power system operation. It provides bulk power transfer over long distances connecting Western and Eastern Java. The power from the 500 kV network is transferred mainly through the 150 kV transmission network to the distribution network. Most of the 70 kV transmission lines are old installations, and PLN has decided not to further expand this voltage level.

The installed capacity of generation in the Java-Bali power system is 10,729 MW. The detailed composition of the generator type is displayed in Table-5.1. The system total peak load by January, 19 1995 was 6,866 MW and 2,450 MVAr [25]. The average daily load factor is 73%, with the morning peak load at 10.00 and the evening peak load at 19.00. The ratio of the morning and the evening peak load is 80%.

Due to low losses, high reliability and capability to transfer large amounts of power the 500 kV transmission networks have a very vital role in the operation of the Java-Bali power system. All the most economic and high capacity generation plants are connected to the 500 kV system. As an example, all the coal fired power stations which are operated at high capacity factors are connected to the 500 kV system. Most gas fired combined cycle plants, which also operate at high capacity factors, due to the nature of take or pay contracts with gas suppliers, are

also connected to the 500 kV network. The total generator capacity directly connected to the 500 kV network is more than 50% of the total system capacity. Therefore the reliability of the Java-Bali power system depends highly on the reliability of the 500 kV network.

Table-5.1:

Power Plant Composition of the Java-Bali Power System [25]

Power Plant	**No. of Units**	**Installed Capacity MW**	**%**
Hydro	86	2026	19
Combined Cycle			
Gas Fired	23	3076	29
Oil Fired	3	329	3
Steam			
Gas Fired	2	400	3
Coal Fired	6	2400	22
Oil Fired	16	1450	14
Geothermal	6	305	3
Gas Turbine			
Gas Fired	6	120	1
Oil Fired	16	531	5
Diesel	17	92	1
TOTAL	181	10729	100

The first 500 kV transmission line was energized in mid 1984, in association with the operation of the first big coal power plant unit (400 MW) in Suralaya, West Java. The first stage of the Java 500 kV network was erected from Suralaya, West Java into Ungaran, Central Java through 3 substations, namely Gandul in Jakarta, Saguling Hydro Power Plant and Bandung in West Java. The development of the Java 500 kV network have extended from Suralaya, West Java to Paiton, East Java in association with the completion of the two large scale coal power plants (2 x 400 MW) in Paiton and 3 blocks of gas fired combined cycle power plants in Gresik, both of them located in East Java, in the year 1993.

The length of the existing Java 500 kV system is 1,499 km. Most of the 500kV transmission connections consist of two single circuit lines. The exceptions are the Cibinong-Saguling, Bandung-Ungaran, and Ungaran-Krian lines, with the total length of 661 km, which are single circuits. However, the construction of the second circuit is expected to commence soon. There are thirteen 500 kV substations which consist of nineteen 500/150 kV transformer units with the total capacity of about 8,500 MVA. The geographical diagram of Java 500 kV system is shown in Figure-5.1. In Figure-5.2 the single line diagram of the Java 500 kV transmission system is shown . The existing Java-Bali system is inter-connected through two circuit 150 kV AC sea bed cables.

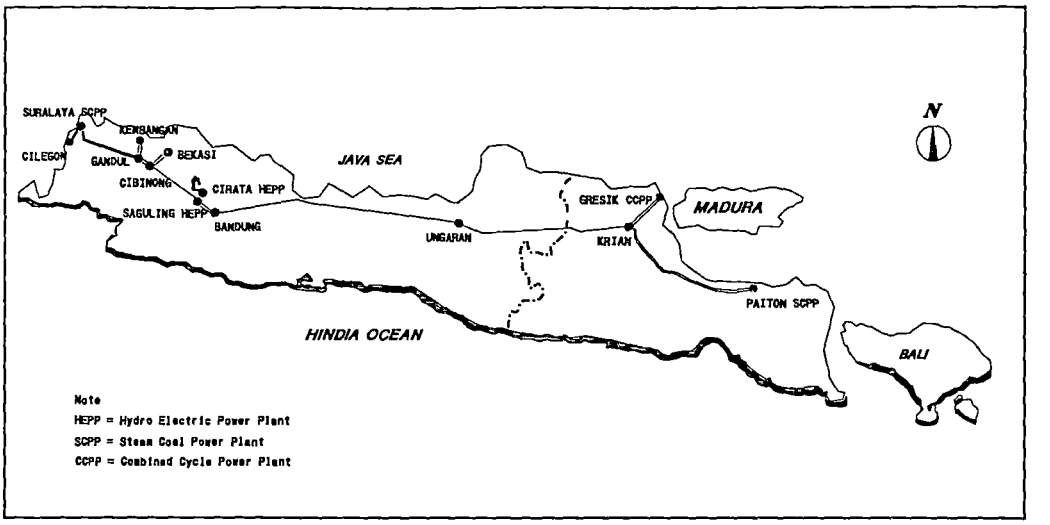

Figure-5.1: Geographical diagram of the Java 500 kV system.

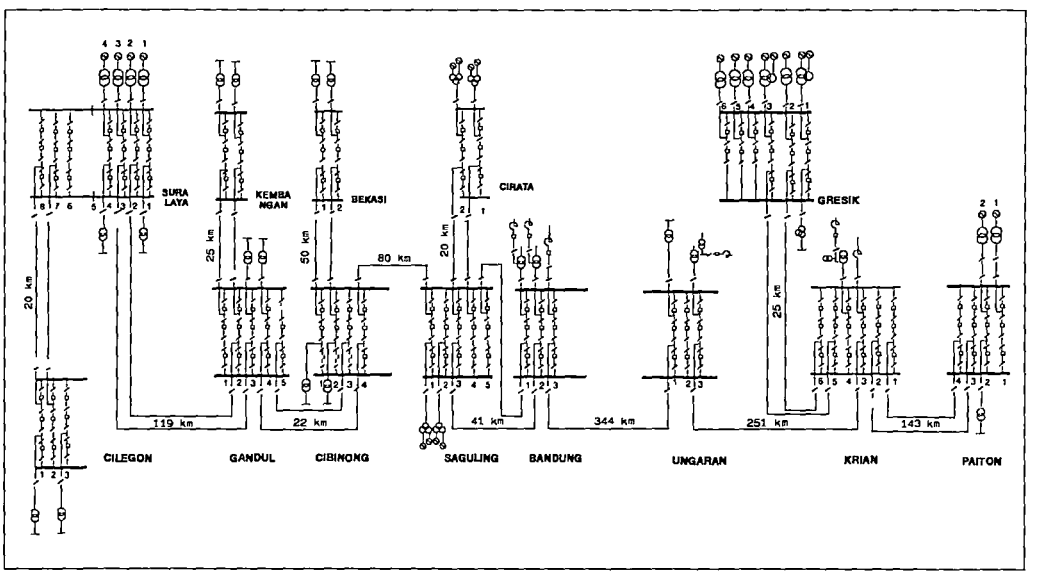

Figure-5.2: Single line diagram of the Java 500 kV system.

5.2 Base Case

The simulation SPAR operation was carried out for a single circuit, 344 km 500 kV transmission line, Bandung-Ungaran the longest line in the Java 500 kV system. Figures 5.1 and 5.2, display the important role of this line on the Java-Bali power system operation. An outage of this line will cause islanding of the Western and the Eastern parts of the system. In the worst condition, under large power

transfer, this outage will cause generation deficiency and possible load shedding in one subsystem, and the overfrequency and possible overvoltages in the other subsystem. Under some conditions this outage may result in the system blackout.

The transposition scheme of the 344 km Bandung-Ungaran line is shown in Figure-5.3.

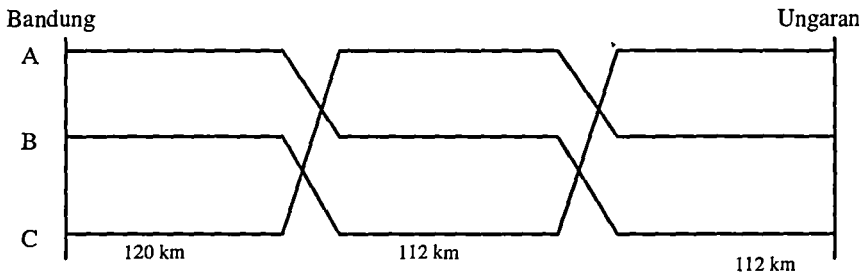

Figure-5.3: Transposition scheme of Bandung-Ungaran line.

The line conductor of Bandung-Ungaran segment consists of two types, namely 120 km of quad Dove and 224 km of quad Gannet conductor. The detailed conductor characteristics are given in Table-5.2, and the unscaled conductors configuration is shown in Figure-5.4.

Table-5.2:

Conductor characteristics

Conductor Type	R dc (Ohm/km)	Radius of Conductor or subconductor (cm)
Dove (ACSR 282 mm^2)	0.1145	1.18
Gannet (ACSR 337.8 mm^2)	0.0955	1.29
Earth wire (Al-St 127 mm^2)	1.8	0.635

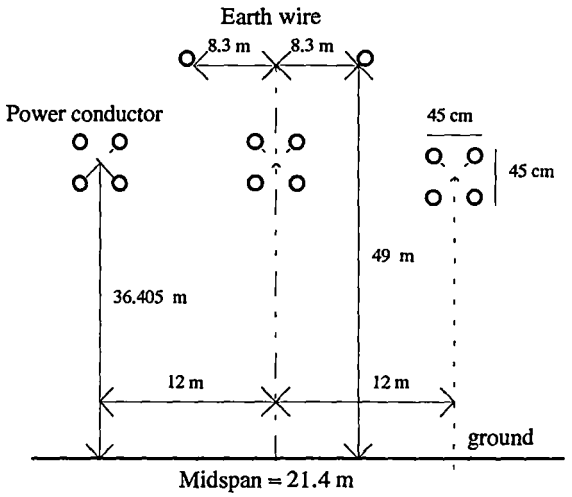

Figure-5.4: Conductors configuration.

Since the monitored parameters associated with SPAR operation, the secondary arc current and the recovery voltage, are in the open faulted phase, the complete system can be reduced to a two buses system [22], namely Bandung and Ungaran. These two buses consist of voltage sources behind a constant short circuit reactance. The short circuit capacity of each bus was calculated with Bandung-Ungaran transmission line open. Under this conditions, the short circuit-equivalent at the Bandung 500 kV bus was 10,572 MVA, equivalent to 0.075 Henry short circuit reactance, and the short circuit-equivalent at the Ungaran 500 kV bus was 4,963 MVA, equivalent to 0.160 Henry short circuit reactance. The short circuit capacity at each bus represented the external system as seen from that particular bus. The reduced system is shown in Figure-5.5. The reduced system reactances were calculated using PSS/E software, developed by Power Technologies Inc.(PTI), USA.

During the simulation it was assumed that there was no existing reactor compensation in Bandung and Ungaran substation. This assumption was made because the installed reactive compensation may be designed for overvoltage compensation or for reactive compensation, which is not included in this simulation.

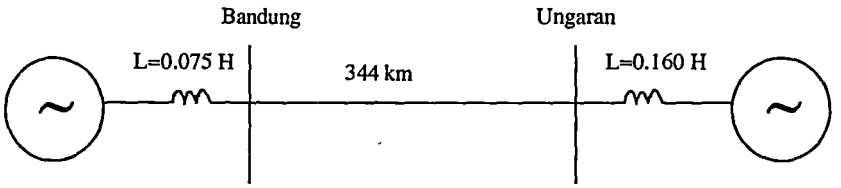

Figure-5.5: The system reduction.

To monitor the steady state secondary arc current and the recovery voltage, a SLG fault was simulated at time 0.1 sec with fault duration of 0.25 sec, and both line end circuit breakers were opened at the same time, 0.16 sec, for the fault location in the middle of the line (zone 1 distance protection). For the fault location at one end of the line, a 0.02 sec time delay was assumed for the far end circuit breaker to open corresponding to transmission delay of an intertrip signal. The steady state secondary arc current was monitored until the extinction of the secondary arc current. The reclosing circuit breaker time delay was set as 0.5 sec for both ends in the case of middle of the line fault location. In the case of SLG fault location at one end of the line, the reclosing time of the far end circuit breaker is 0.52 seconds. The steady state recovery voltage was monitored after the extinction of the secondary arc current and until the reclosing of the line circuit breakers. The simulation was repeated for three values of arc resistance, namely, 1 Ohm, 10 Ohm and 100 Ohm. The simulation indicated that the effect of these different arc resistance values on the results is negligible.

Figure-5.6 shows that the steady state secondary arc current for an uncompensated line was around 53 A, and the recovery voltage was 41 kV. These results were almost the same as the result of hand calculations presented in the Appendix-3. Based on laboratory test results, if the duration of the secondary arc is to be limited to about 0.5 sec, then the magnitude of the secondary arc current should not be larger than 20 A and the recovery voltage should be less than 50 kV. The gradient recovery voltage was calculated by dividing the value of the recovery voltage from

the simulation by the assumed length the secondary arc of 2.6 m, the distance between the arcing horns of insulator string. Based on the relationship between the gradient recovery voltage and the secondary arc current (Figure-A2.2), the duration of the secondary arc, for the line without compensation scheme, was estimated as 1.52 sec. The maximum practical value of the SPAR dead time is about 0.7 sec, assuming 0.5 sec required extinction of the secondary arc and 0.2 sec for de-ionisation of the arc path. Therefore, without a compensation scheme, the SPAR operation of the 500kV Bandung-Ungaran transmission line, will be unsuccessful.

Installation of a four-legged reactor in Ungaran, designed for a 60% compensation factor which results in 3×1262 Ohm phase reactances and 645 Ohm neutral reactance (Appendix-3); results in reduction of the secondary arc current to 7 A and corresponding decrease of the recovery voltage to 17.3 kV.

If a three-legged reactor with 3×1262 Ohm phase reactances but without neutral reactor was installed in Ungaran the secondary arc current would be the same as for the uncompensated line. However, due to the resonance of the reactor and the line capacitance, the recovery voltage increased to 151 kV (Figure-5.7).

The summary of simulation results are shown in Table-5.3.

Table-5.3: The detailed SPAR results

	The steady state secondary arc current (A)	The recovery voltage (kV)	The gradient recovery voltage (kV/m)	Time extinction (sec)
Without Reactor	53	41	16	1.52
3-legged Reactor	53	151	58	>2
4-legged Reactor	6.9	17.3	7	0.1

5.3 Sensitivity Analysis

The sensitivity analysis was carried out to investigate the impact of various factors on parameters affecting SPAR performance: the power frequency secondary arc current and the steady state recovery voltage.

The effect of line transposition

Figure-5.8 shows the secondary arc current and the recovery voltage for a SLG fault located in different phases of an untransposed line. The figure indicates that the magnitude of the secondary arc current and the recovery voltage for a fault on the middle phase is higher than the respective values for fault placed in the outer phase. Figure-5.9 displays the same quantities for a transposed line. In a transposed line, the secondary arc current and the steady state recovery voltage are the same for a SLG fault placed in any phase.

Figure-5.10 shows the comparison of the effectiveness of a four-legged reactor compensation for a transposed line and an untranposed line. The four-legged reactor can effectively compensate the interphase capacitance of a transposed line, but does not compensate the mutual capacitive coupling of the untransposed line.

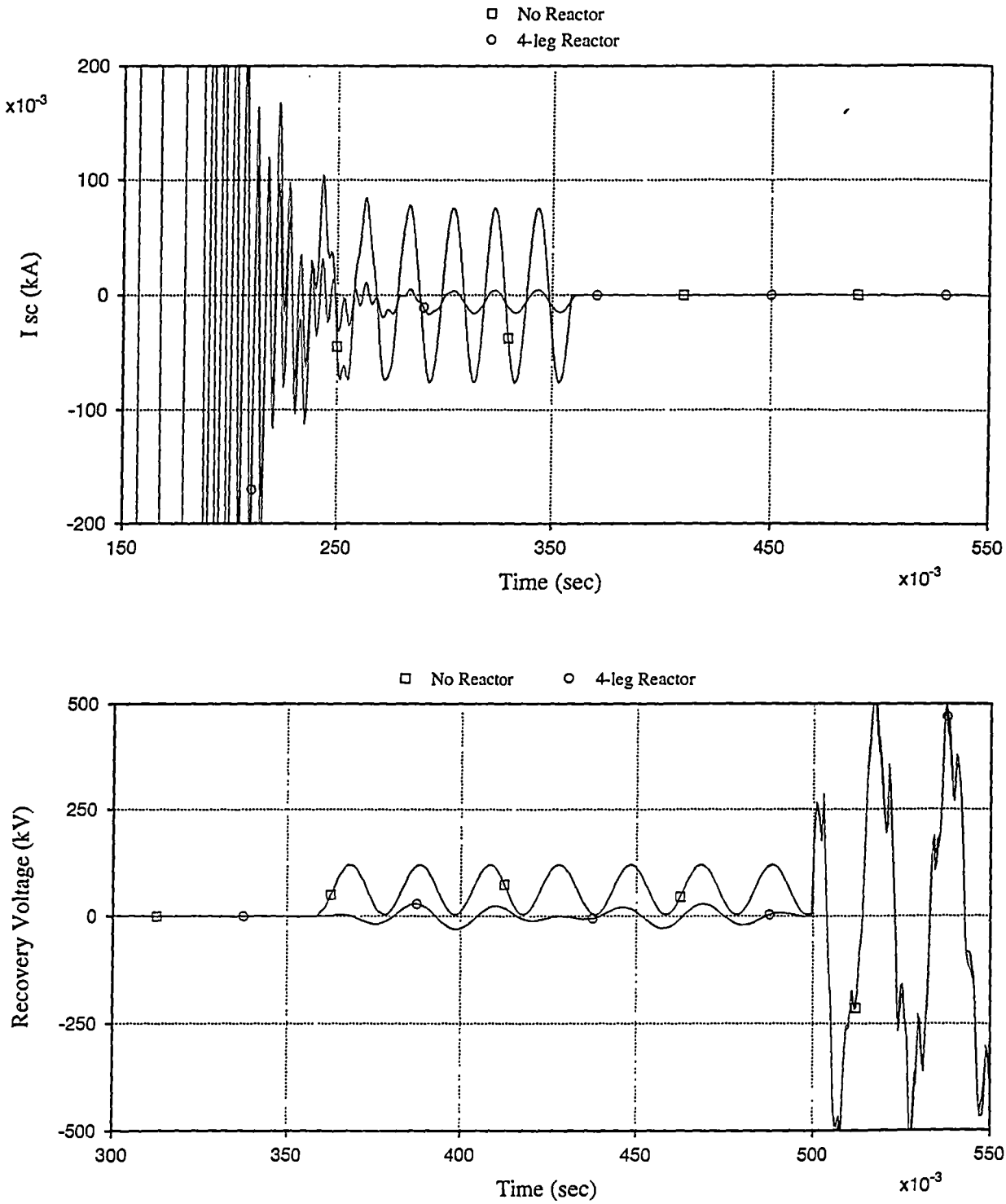

Figure-5.6: The comparison of the secondary arc current and the recovery voltage for an uncompensated and compensated (4-legged reactor) transposed line.

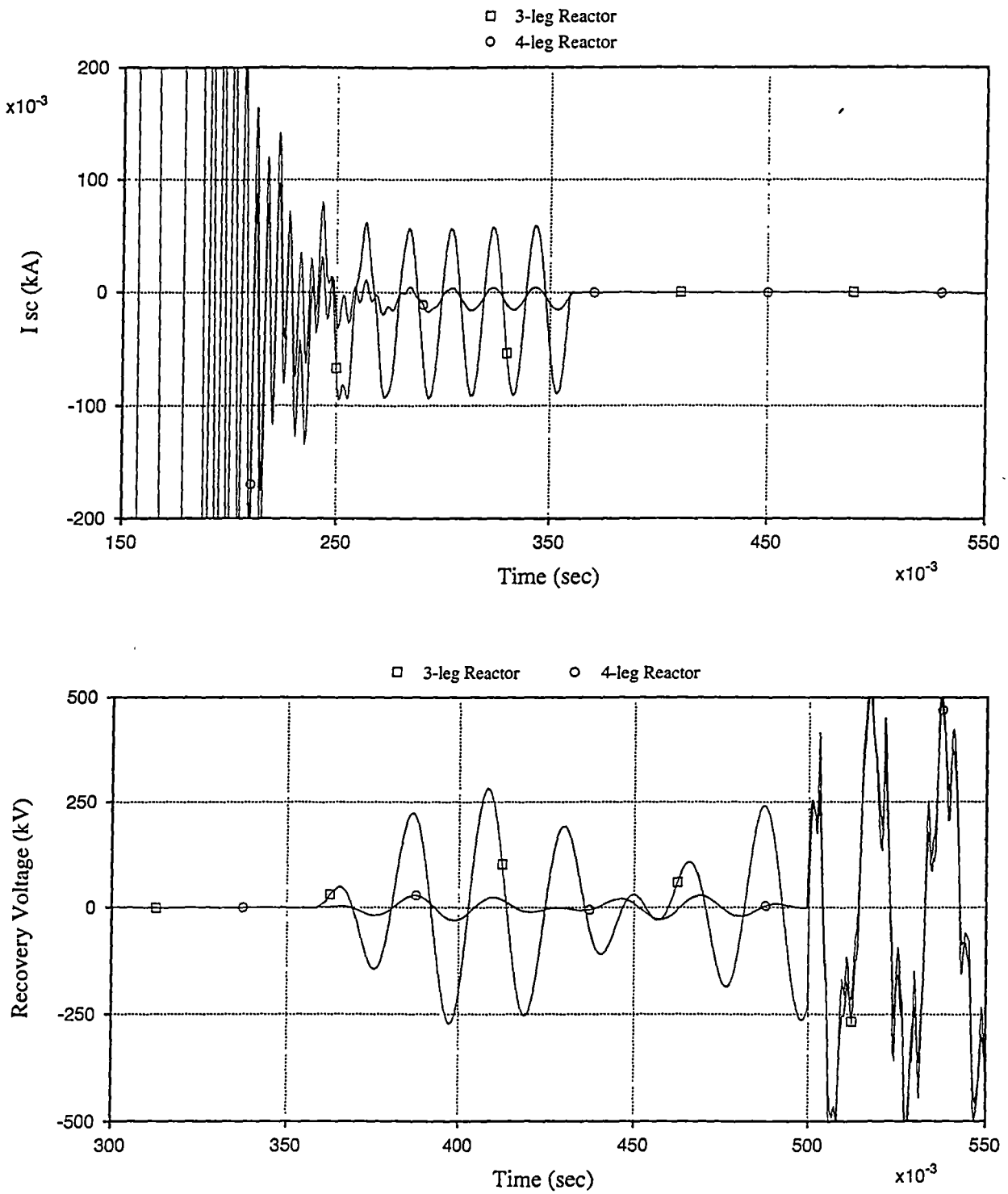

Figure-5.7: The comparison of the secondary arc current and the recovery voltage for a 3-legged and a 4-legged reactor compensation of a transposed line.

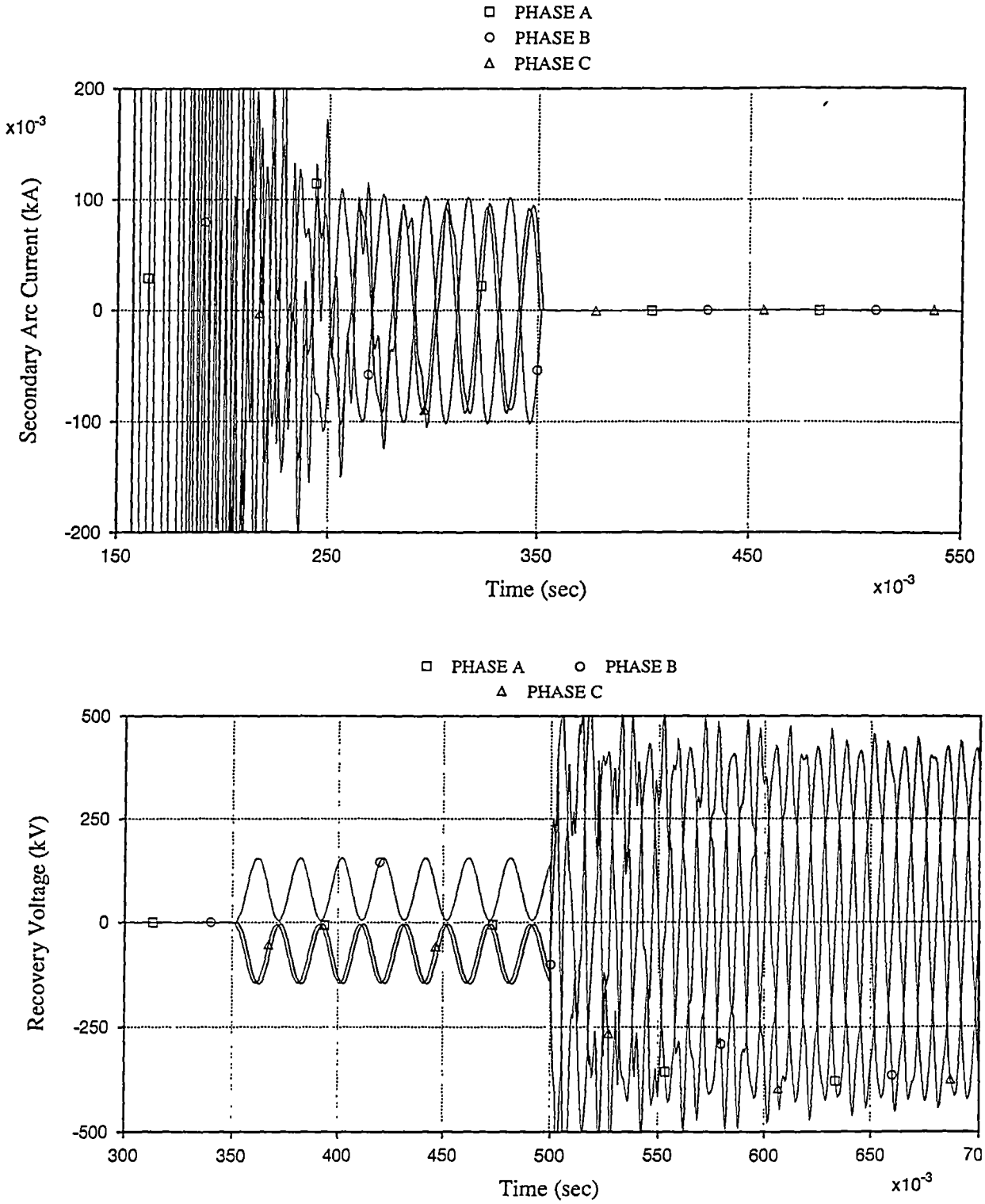

Figure-5.8: The secondary arc current and the recovery voltage for a SLG fault placed in different phases of an untransposed line.

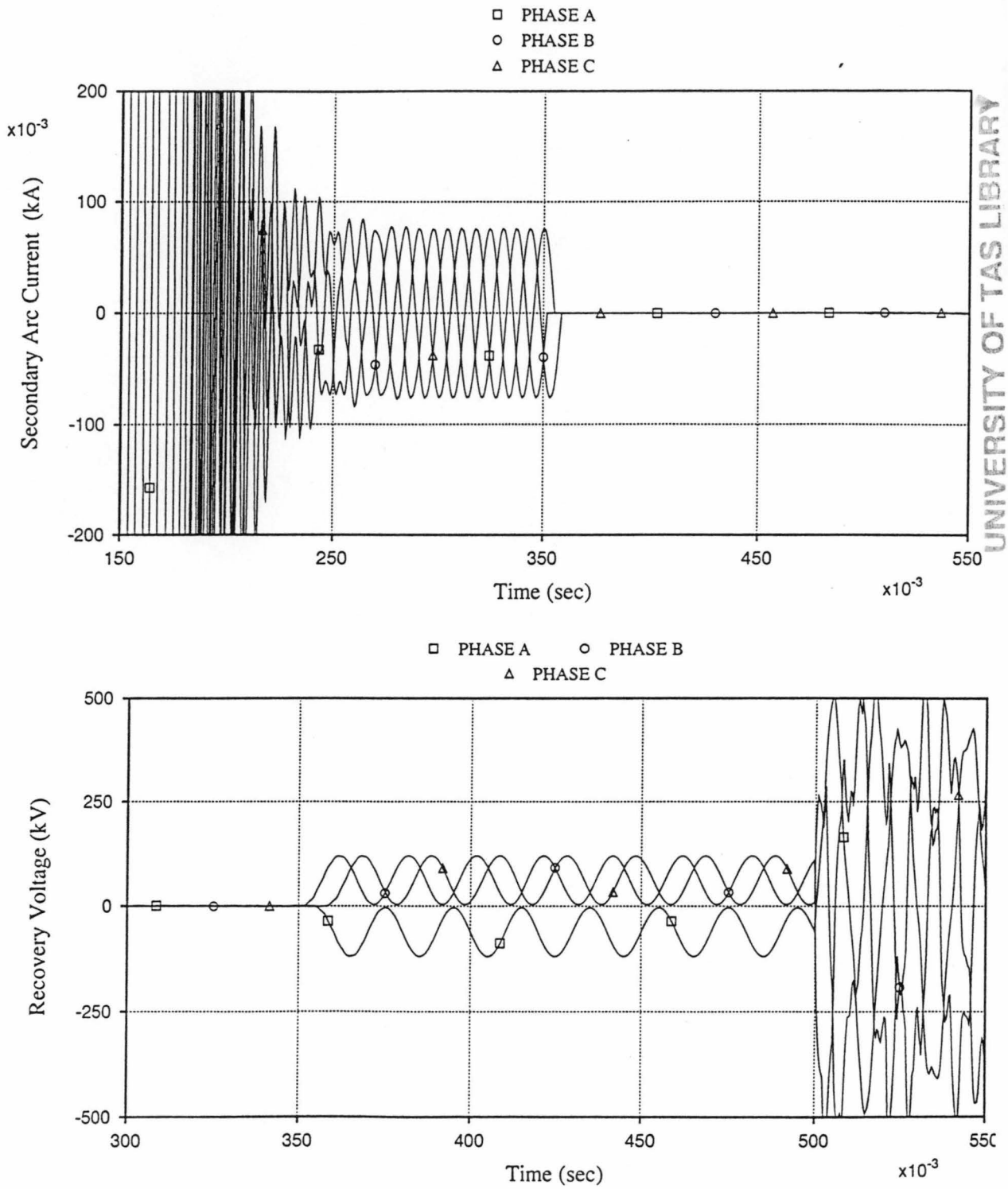

Figure-5.9: The secondary arc current and the recovery voltage for a SLG fault placed in different phases of a transposed line.

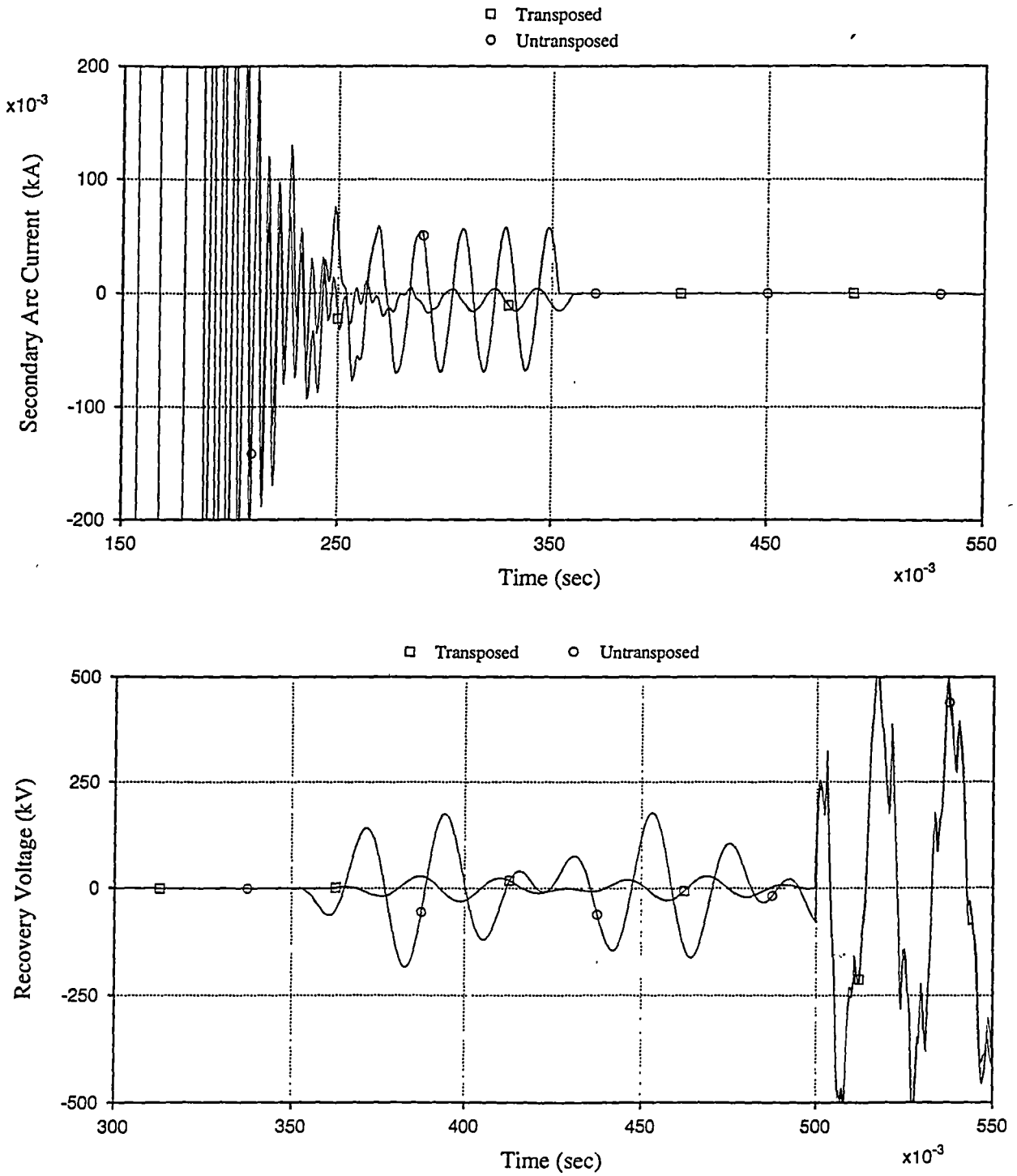

Figure-5.10: The comparison of the effectiveness of a 4-legged reactor to compensate a transposed and an untranposed line.

The effect of transmission line length

Figure-5.11 shows the effect of line length in SPAR operations for a transposed line. By doubling the transmission line length, from 344 km to 688 km, the secondary arc current approximately increases two times, from 53 A to 129 A. However, the recovery voltage remains almost the same, 41 kV. This result agrees with equation (3.5) and equation (3.9).

The effect of fault location

Figure-5.12 shows the secondary arc current and the recovery voltage for a SLG fault located at both ends of the line and in the middle of the line for an unloaded transmission line. The secondary arc current and the recovery voltage in this case are mainly induced by the capacitive mutual coupling, which has the same value regardless of the fault location.

Figure-5.13 shows the secondary arc current and the recovery voltage for the 700 MW prefault power flow, which was achieved by forcing a 30 degree phase shift between the two voltage sources. The secondary arc current and the recovery voltage for SLG fault located at both ends were greater than for SLG fault located at the midpoint of the line. This result, for the fault placed in the middle of line, shows that the inductive mutual coupling effects in both sections of the line cancelled each other.

The effect of prefault line loading

Figure-5.14 shows the impact of prefault line loading on a SPAR operation. The secondary arc current increased from 6.9 A for no load conditions to 17.3 A for a 500 MW prefault power flow forced by a 20 degree phase shift between two voltage sources.

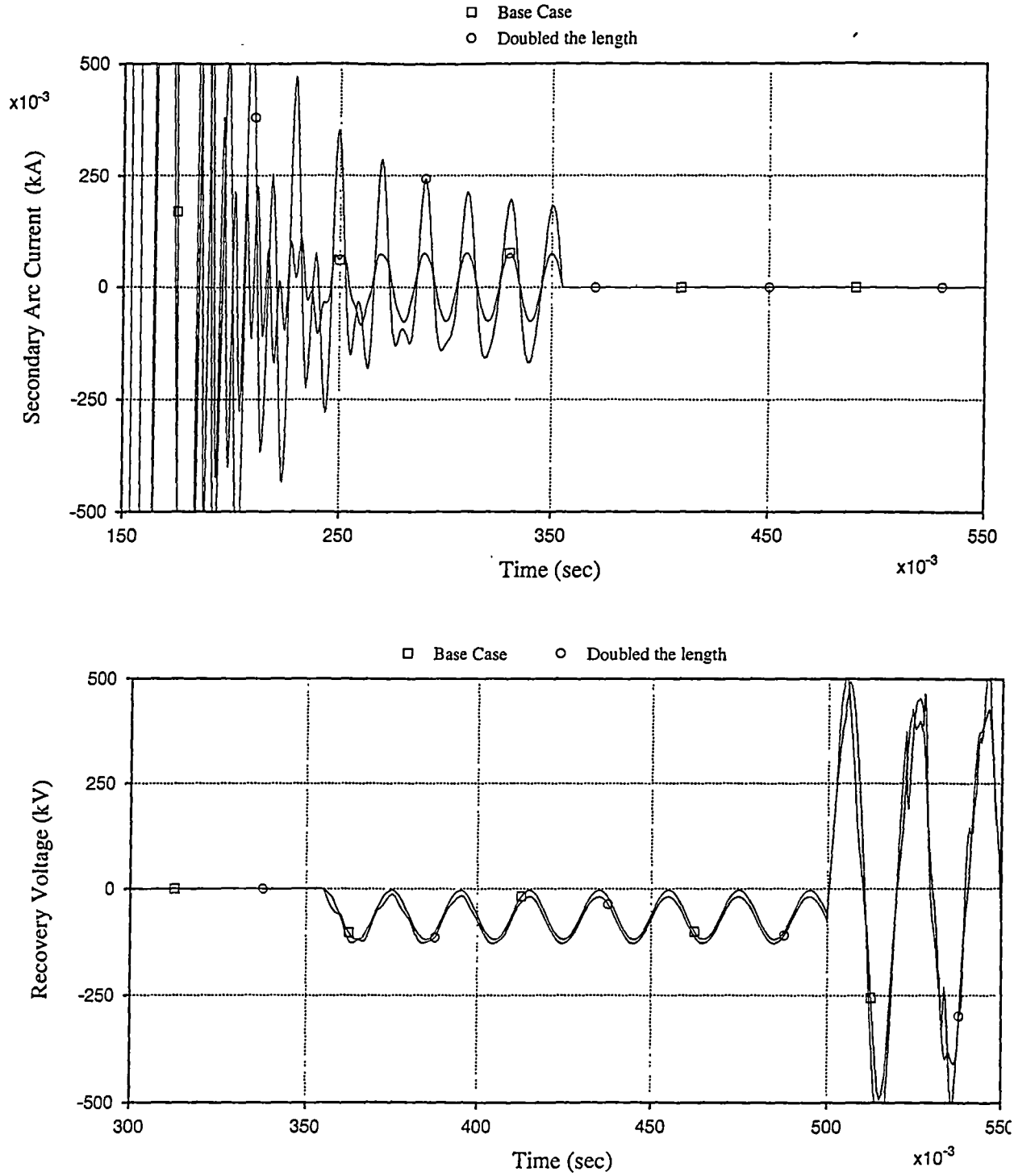

Figure-5.11: The effect of line length on the secondary arc current and the recovery voltage of a transposed line.

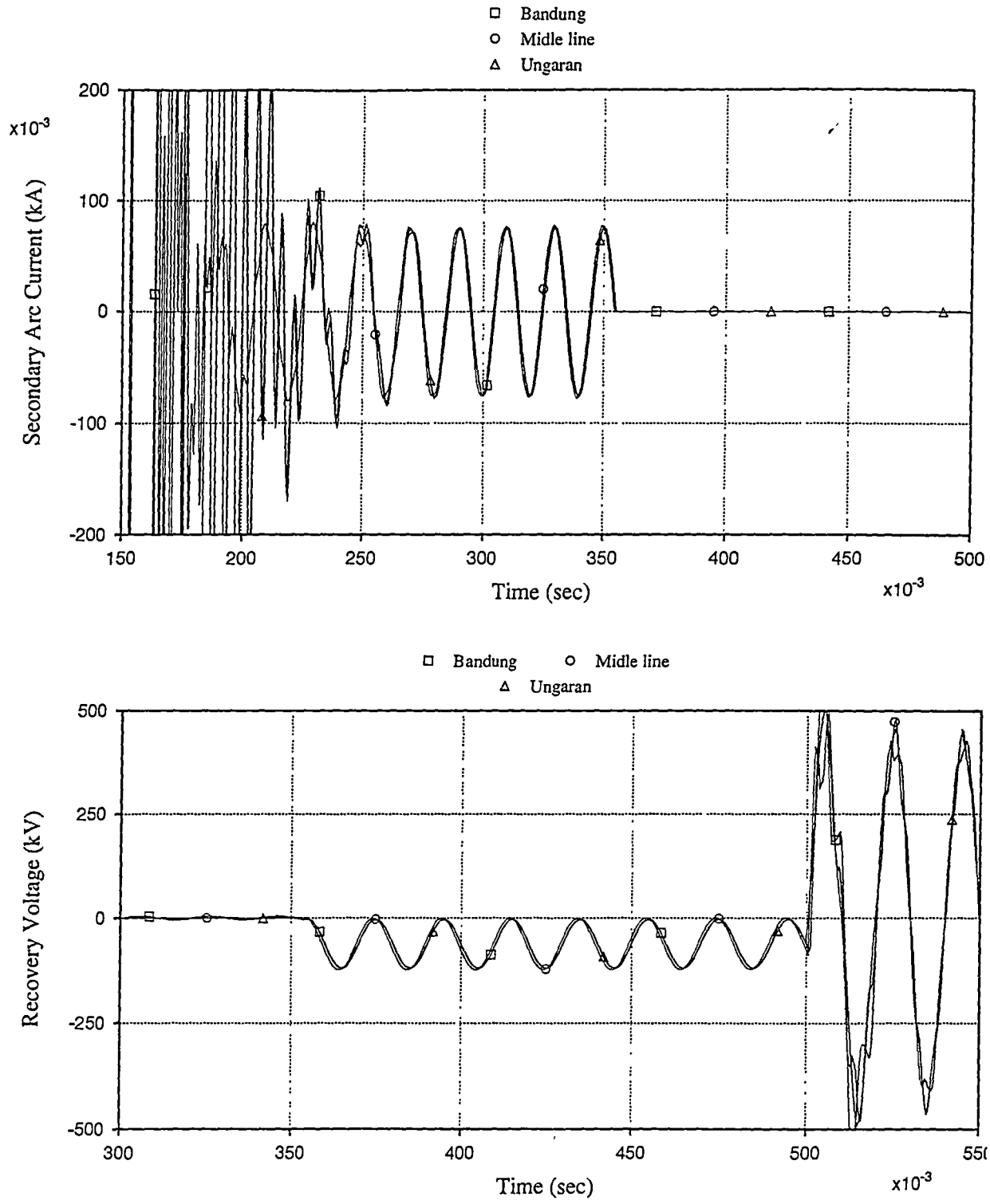

Figure-5.12: The effect of fault location on the secondary arc current and the recovery voltage of an unloaded, transposed line.

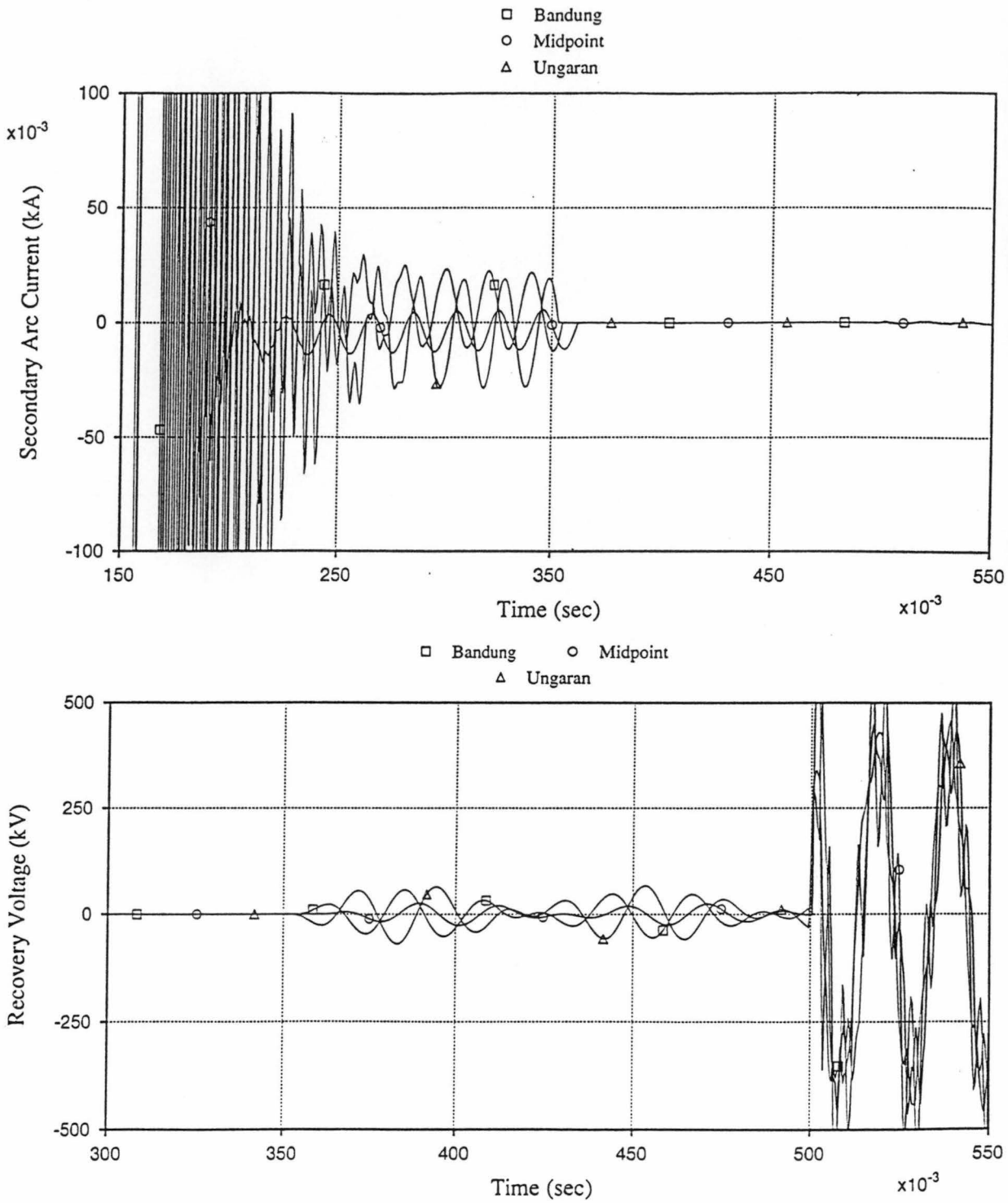

Figure-5.13: The effect of fault location on the secondary arc current and the recovery voltage of a transposed line with the 700 MW prefault line loading.

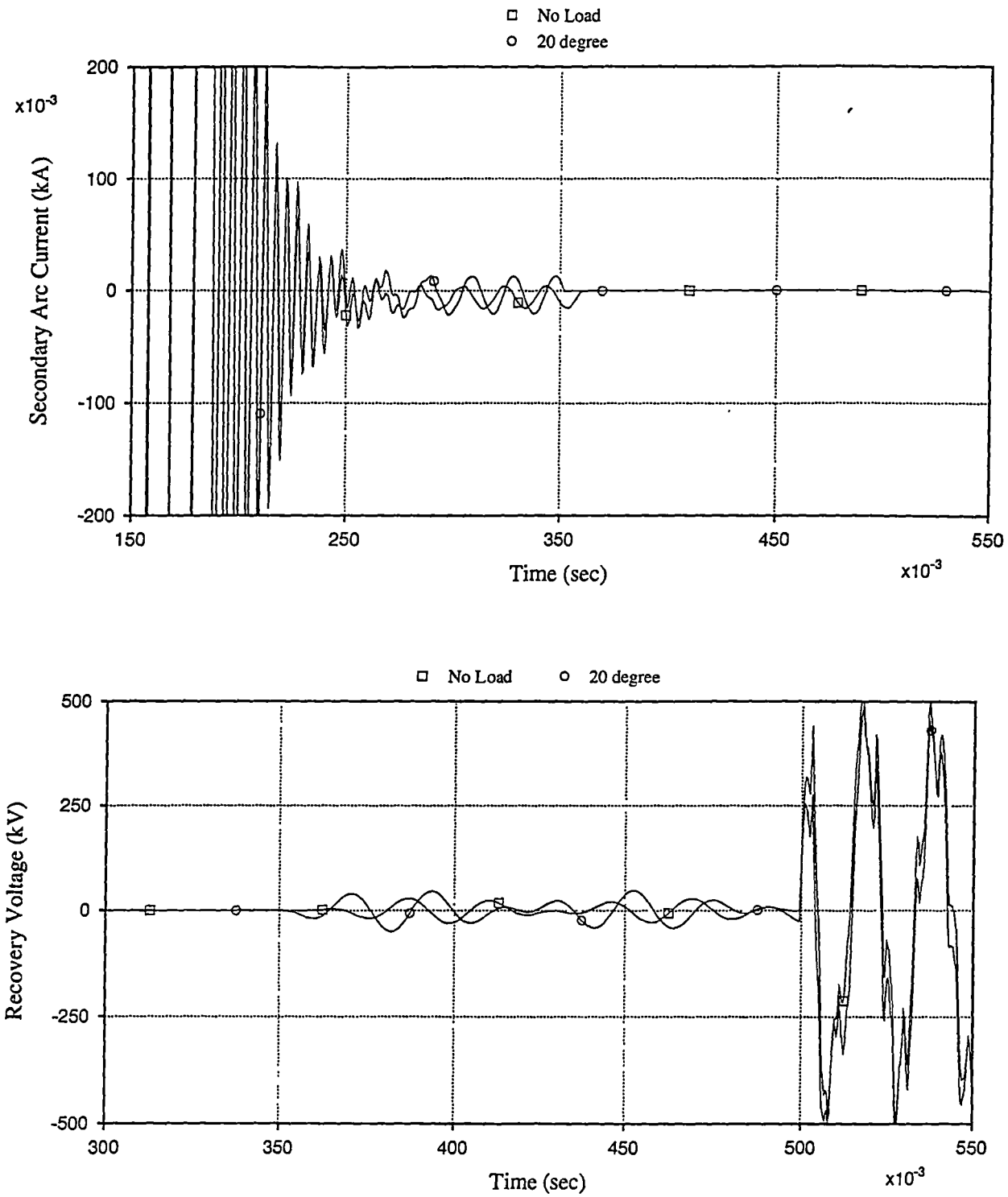

Figure-5.14: The effect of prefault line loading on the secondary arc current and the recovery voltage of a transposed line.

CHAPTER 6

CONCLUSIONS

A successful SPAR operation effectively increases system stability. To ensure a successful SPAR operation in a long 500kV transmission line there are three compensation methods based on neutralizing mutual capacitive coupling, speeding up the secondary arc discharge and natural arc extinction.

The results of staged fault tests and laboratory tests, indicate a strong relationship between the secondary arc duration and values of the secondary arc current and the recovery voltage. Field practice indicates that if the secondary arc current does not exceed 20 A and the recovery voltage is less than about 50 kV, the duration of secondary arc extinction is expected within 0.5 sec. The secondary arc duration can be determined by using Figure-A2.2 which defines this value as a function of the gradient recovery voltage and the secondary arc current.

Based on the simulation of the steady state secondary arc current and the steady state recovery voltage during SPAR operation on the 344 km single circuit 500 kV transmission line with a flat quad conductor configuration, it can be concluded that:

1. The secondary arc current and the recovery voltage of a transposed line do not depend on the location of the faulted phase. For an untransposed line, the secondary arc current and the recovery voltage for a fault placed on the middle phase is higher than in case of a fault on the outer phases. This is caused by unequal mutual capacitance between phases.

2. There is a linear relationship between line length and the magnitude of the secondary arc current. If the line length increases, the secondary arc current

also increases. Therefore, to ensure a successful SPAR operation of the 500kV transmission line a compensation scheme must be applied if the line length exceed about 100 km.

3. The magnitude of the secondary arc current due to the mutual inductive coupling depends on the fault location and the prefault line loading.

4. The impact of the mutual inductive coupling is negligible if a SLG fault occurs in the midpoint of the line.

5. A four-legged reactor effectively compensates the secondary arc current and reduces the recovery voltage of a transposed line, but this arrangement is not effective for an untransposed line.

6. A three-legged reactor does not compensate either the secondary arc current or the recovery voltage. This arrangement may be dangerous under SPAR operation when the reactor may resonate with the line capacitance to significantly increase the recovery voltage.

The simulation results are consistent with theoretical background. In this thesis the design of a compensation scheme for the 500 kV transmission line was carried out exclusively to illustrate effectiveness of SPAR operation. However, the design of practical compensation scheme would also include analysis of the system performance under overvoltage conditions caused by line energization or load rejection which was outside the scope of this study.

REFERENCES

1. Arrillaga, J., Arnold, C.P., and Harker, B.J., *Computer Modelling of Electrical Power Systems*, John Willey & Sons, Chichester,(1983).
2. Dommel, Herman. W, *Electro Magnetic Transient Program Reference Manual (EMTP Theory Book),* BPA,(August 1986).
3. Edwards, L., Chadwick, J.W., Jr., Riesch, H.A., and Smith, L.E., *Single-pole switching on TVA's Paradise-Davidson 500 kV line design concepts and staged fault test result*, IEEE Trans. PA&S, 90, pp. 2436-2450,(Nov./Dec. 1971).
4. Fakheri, A., Grzan, J., and Shperling, B.R., *The use of reactor switching in single phase switching*, CIGRE, Paper 13-06,(1980).
5. Fakheri, A.J., Shuter, T.C., Schneider, J.M., and Shih, C.H., *Single phase switching tests on the EAP 765 kV system extinction time for large secondary arc currents*, IEEE Trans. PA&S, 102, pp. 2775-2783,(August. 1983).
6. Greenwood, Allan., *Electrical Transients in Power Systems*, Willey-Interscience, New York,(1971).
7. Hasibar, R.M., Legate, A.C., Brunke, J., and Peterson, W.G., *The application of high-speed grounding switches for single-pole reclosing on 500 kV power systems*, IEEE Trans. PA&S, 100, pp. 1512-1515,(April 1981).
8. Haubrich, H.J., Hosemann, G., and Thomas, R., *Single-phase auto-reclosing in EHV systems*, CIGRE, Paper 31-09,(1974).
9. IEEE Panel Discussion Report, *Single-pole switching for stability and reliability,* IEEE Trans. on Power Systems, 1, pp. 25-36,(May 1986).
10. IEEE Committee Report, *Single phase tripping and auto reclosing of transmission lines*, IEEE Trans. on Power Delivery, 7, pp. 182-192,(Jan 1992).

11. Johns, A.T., Al-Rawi, A.M., *Digital simulation of EHV systems under secondary arcing conditions associated with single-pole autoreclosure*, IEE Proc. Pt. C, 129, pp.49-58,(March 1982).

12. Kappenman, J.G., Sweezy, G.A., Koschik, V., and Mustaphi, K.K., *Staged fault tests with single phase reclosing on the Winnipeg-Twin Cities 500 kV interconnections*, IEEE Trans, PA&S, 101, pp. 662-673,(March 1982).

13. Kimbark, E.W., *Suppression of ground-fault arcs on single-pole-switched EHV lines by shunt reactors*, IEEE Trans. PA&S, 83, pp. 285-290, (March 1964).

14. Knudsen, N., *Single phase switching of transmission lines using reactors for extinction of the secondary arcs*, CIGRE, Paper 310,(1962).

15. Lambert, S.R., Kuschik, V., and Wood, C.E., *Long line single-phase switching transient and their effect on station equipment*, IEEE Trans. PA&S, 97, pp. 857-865,(May/June 1978).

16. Manitoba HVDC Research Centre, *EMTDC User's Manual*,(1988).

17. Merz and McLellan, and PT Hasfarm Dian Konsultan, *Power system and fast transient studies for second 500 kV Bandung Selatan-Ungaran-Krian line circuits in Java*, Vol 3,(November 1992)

18. Perry, D.E., Hasibar, R.M., Ware, B.J., Fakheri, A.J., Chadwick, J.W., and Bayless, R.S., *Investigation and evaluation of single-phase switching on EHV network in the United States*, CIGRE, Paper 39-08,(1984).

19. Peterson, H.A., and Dravid, N.V., *A method for reducing dead time for single-phase reclosing in EHV transmission*, IEEE Trans. PA&S, 88, pp. 286-292,(April 1969).

20. Scherer, H.N., Shperling, B.R., Chadwick, J.W., Belyakov, N.N., Rashkes, V.S., and Khoetsian, K.V., *Single phase switching tests on 765 kV and 750 kV transmission lines*, IEEE Trans PA&S, 104, pp. 1537-1548,(June 1985).

21. Sekine, Y., Ichida, Y., Nakamura, A., and Suzuki, H., *Asymmetrical four-legged reactor extinguishing secondary arc current for high-speed reclosing on UHV system,* CIGRE, Paper 38-03,(1984).

22. Shperling, B.R., Fakheri, A., and Ware, B.J., *Compensation scheme for single-pole switching on untransposed transmission lines*, IEEE Trans. PA&S, 97, pp. 1421-1429,(July/Aug. 1978).

23. Shperling, B.R., and Fakheri, A., *Single-phase switching parameters for untransposed HV transmission lines*, IEEE Trans. PA&S, 98, pp. 643-654,(March/April 1979).

24. Shperling, B.R., Fakheri, A.J., Shih, S.H., and Ware, B.J., *Analysis of single phase switching field tests on AEP 765 kV system*, IEEE Trans. PA&S, 100, pp. 1729-1735,(April 1981).

25. Situmeang, Hardiv. H, *Java-Bali Power System present status, problem solving strategies and progress*, PT PLN(PERSERO),(1995).

APPENDIX 1

TRANSMISSION LINE PARAMETERS

Transmission line parameters are calculated from the tower configuration, conductors, the effect of ground current and earth wires. These parameters are expressed as a series of impedance and shunt admittance per unit length of the line.

Series Impedance

A longitudinal diagram of a single circuit three-phase transmission line with a ground wire is displayed in Figure-A1.1 [1].

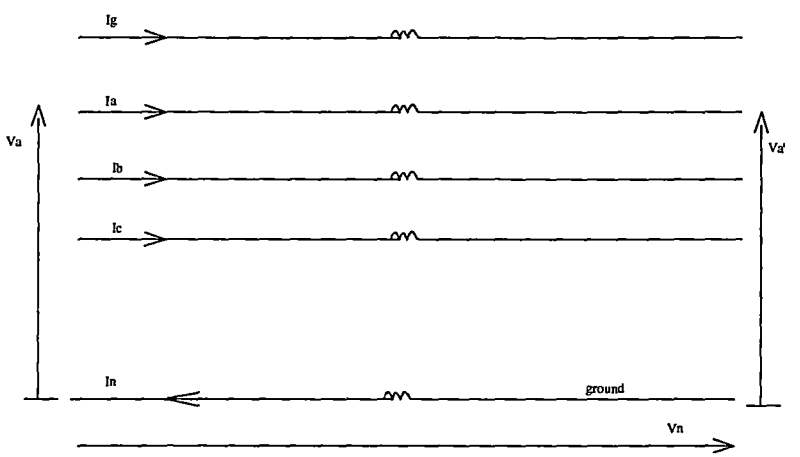

Figure-A1.1: Series impedance diagram of a three-phase transmission line.

The voltage drop on phase 'a' along the line can be written as follows:

$$V_a - V_a' = I_a(R_a + j\omega L_{aa}) + I_b(j\omega L_{ab}) + I_c(j\omega L_{ac}) + I_g(j\omega L_{ag}) - I_n(j\omega L_{an}) + V_n \quad \text{(A1.1)}$$

Where the entries of self and mutual series impedance are:

$$Z_{ii} = R_i + j\omega L_{ii} \quad \text{(A1.2a)}$$

$$Z_{ij} = j\omega L_{ij}; \quad i \neq j \quad \text{(A1.2b)}$$

$$L_{ij} = \frac{\mu}{2\pi}\ln\frac{1}{D_{ij}}; \quad i,j = a,b,c,g,n$$

$$D_{ii} = r_i' = re^{-1/4} = GMR_i$$

r_i is radius of the conductor.

μ is permeability constant (in air $\mu = 4\pi 10^{-7} H/m$)

Expressions for the neutral voltage and current are as follow:

$$V_n = I_n(R_n + j\omega L_{nn}) - I_a(j\omega L_{an}) - I_b(j\omega L_{bn}) - I_c(j\omega L_{cn}) - I_g(j\omega L_{gn}) \qquad \text{(A1.3)}$$

$$I_n = I_a + I_b + I_c \qquad \text{(A1.4)}$$

By substituting (A1.3) and (A1.4) into (A1.1) and defining the voltage drop in the phase 'a' as ΔV_a, then :

$$\Delta V_a = I_a(R_a + j\omega L_{aa} - 2j\omega L_{an} + R_n + j\omega L_{nn}) + I_b(j\omega L_{ab} - j\omega L_{bn} - j\omega L_{an} + R_n + j\omega L_{nn}) + I_c(j\omega L_{ac} - j\omega L_{cn} - j\omega L_{an} + R_n + j\omega L_{nn}) + I_g(j\omega L_{ag} - j\omega L_{gn} - j\omega L_{an} + R_n + j\omega L_{nn}) \qquad \text{(A1.5)}$$

or in the simple form:

$$\Delta V_a = Z_{aa-n}I_a + Z_{ab-n}I_b + Z_{ac-n}I_c + Z_{ag-n}I_g$$

In the same way the voltage drop of the other conductors can be formulated and the results can be written in matrix form as follows:

$$\begin{bmatrix} \Delta V_a \\ \Delta V_b \\ \Delta V_c \\ \Delta V_g \end{bmatrix} = \begin{bmatrix} Z_{aa-n} & Z_{ab-n} & Z_{ac-n} & Z_{ag-n} \\ Z_{ab-n} & Z_{bb-n} & Z_{bc-n} & Z_{bg-n} \\ Z_{ac-n} & Z_{bc-n} & Z_{cc-n} & Z_{cg-n} \\ Z_{ag-n} & Z_{bg-n} & Z_{cg-n} & Z_{gg-n} \end{bmatrix} \begin{bmatrix} I_a \\ I_b \\ I_c \\ I_g \end{bmatrix} \qquad \text{(A1.6)}$$

The element of self and mutual impedance can be formulated by substituting (A1.2a) and (A1.2b) into (A1.5).

$$Z_{aa-n} = R_a + R_n + j\frac{\omega\mu}{2\pi}\ln\frac{D_{na}^2}{r_a' r_n'}$$

$$Z_{bb-n} = R_b + R_n + j\frac{\omega\mu}{2\pi}\ln\frac{D_{nb}^2}{r_b' r_n'}$$

$$Z_{cc-n} = R_c + R_n + j\frac{\omega\mu}{2\pi}\ln\frac{D_{nc}^2}{r_c' r_n'}$$

$$Z_{ab-n} = R_n + j\frac{\omega\mu}{2\pi}\ln\frac{D_{na}D_{nb}}{D_{ab}\, r_n'}$$

$$Z_{bc-n} = R_n + j\frac{\omega\mu}{2\pi}\ln\frac{D_{bn}D_{cn}}{D_{bc}\, r_n'}$$

$$Z_{ac-n} = R_n + j\frac{\omega\mu}{2\pi}\ln\frac{D_{an}D_{cn}}{D_{ac}\, r_n'}$$

$R_n = 9.869x10^{-7} f\ \Omega / m$ is the earth resistance, f = frequency.

The ground wire elements can be eliminated by partition (A1.6).

$$\begin{bmatrix} \Delta V_{abc} \\ \Delta V_g \end{bmatrix} = \begin{bmatrix} Z_A & Z_B \\ Z_C & Z_D \end{bmatrix} \begin{bmatrix} I_{abc} \\ I_g \end{bmatrix} \qquad \text{(A1.7)}$$

By considering $\Delta V_g = 0$, then $[\Delta V_{abc}] = [Z_{abc}][I_{abc}]$ (A1.8).

Where $[Z_{abc}] = [Z_A] - [Z_B][Z_D]^{-1}[Z_C]$. (A1.9)

Elements of series impedance matrix are usually not balanced, neither the diagonal of the off-diagonal element has a common value.

$$[Z_{abc}] = \begin{bmatrix} Z_{aa} & Z_{ab} & Z_{ac} \\ Z_{ab} & Z_{bb} & Z_{bc} \\ Z_{ac} & Z_{bc} & Z_{cc} \end{bmatrix}$$

The lines become approximately balanced if the line is transposed as shown in Figure-A1.2.

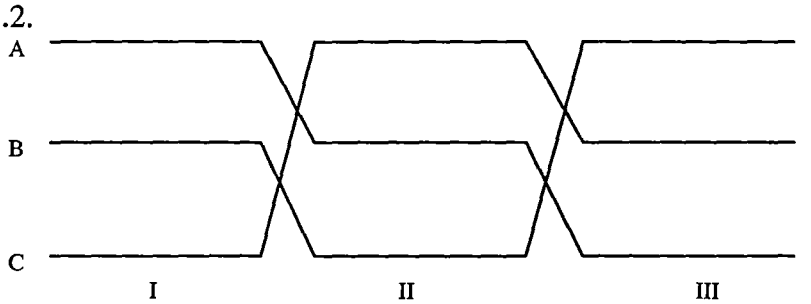

Figure-A1.2: Transposition of a single circuit three-phase line.

If the transposition segment is much shorter than the wavelength then the series impedance can be averaged as follows:

$$Z_s = \tfrac{1}{3}(Z_{aa} + Z_{bb} + Z_{cc}) \quad \text{(A1.10)}$$

$$Z_m = \tfrac{1}{3}(Z_{ab} + Z_{bc} + Z_{ac}) \quad \text{(A1.11)}$$

Therefore the series impedance matrix of a fully transposed line is:

$$[Z_{abc}] = \begin{bmatrix} Z_s & Z_m & Z_m \\ Z_m & Z_s & Z_m \\ Z_m & Z_m & Z_s \end{bmatrix} \quad \text{(A1.12)}$$

The symmetrical component of the series impedance is :

$$[Z_{012}] = [T]^{-1}[Z_{abc}][T] \quad \text{(A1.13)}$$

Where T is a transformation matrix. For a transposed line, the symmetrical component impedance is :

$$[Z_{012}] = \begin{bmatrix} Z_0 & 0 & 0 \\ 0 & Z_1 & 0 \\ 0 & 0 & Z_2 \end{bmatrix} \quad \text{(A1.14)}$$

where

$$Z_0 = Z_s + 2Z_m$$
$$Z_1 = Z_2 = Z_s - Z_m \quad \text{(A1.15)}$$

Conversely

$$Z_m = \tfrac{1}{3}(Z_0 - Z_1)$$
$$Z_s = \tfrac{1}{3}(Z_0 + 2Z_1) \qquad \text{(A1.16)}$$

Shunt Capacitance

Based on Figure-A1.3, the relation between the line conductor potentials and the conductor charges can be formulated in matrix equation:

$$\begin{bmatrix} V_a \\ V_b \\ V_c \\ V_g \end{bmatrix} = \begin{bmatrix} P_{aa} & P_{ab} & P_{ac} & P_{ag} \\ P_{ab} & P_{bb} & P_{bc} & P_{bg} \\ P_{ac} & P_{bc} & P_{cc} & P_{cg} \\ P_{ag} & P_{bg} & P_{cg} & P_{gg} \end{bmatrix} \begin{bmatrix} Q_a \\ Q_b \\ Q_c \\ Q_g \end{bmatrix} \qquad \text{(A1.17)}$$

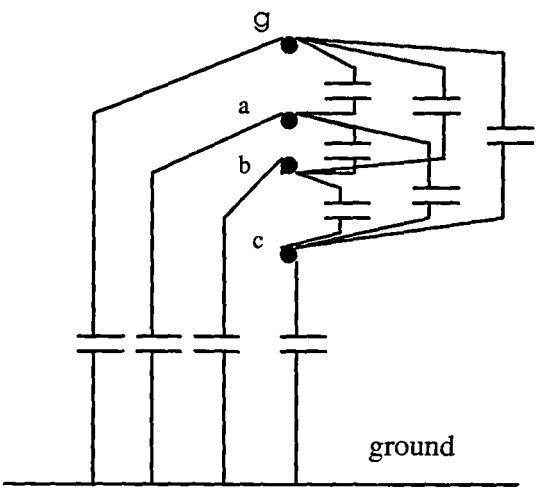

Figure-A1.3: Shunt admittance equivalent of a three-phase line.

Element of the Maxwell's potential coefficient matrix is :

$$P_{ij} = \frac{1}{2\pi\varepsilon} \ln\frac{H_{ij}}{D_{ij}}$$

where ε is the permitivity constant (in air $\varepsilon = 8.854x10^{-12}\,F/m$); H_{ij} is the distance between conductor i and the image of conductor j; D_{ij} is the distance between conductor i and conductor j.

The ground wire elements can be eliminated by partition (A1.17).

$$\begin{bmatrix} V_{abc} \\ V_g \end{bmatrix} = \begin{bmatrix} P_A & P_B \\ P_C & P_D \end{bmatrix} \begin{bmatrix} Q_{abc} \\ Q_g \end{bmatrix} \qquad \text{(A1.18)}$$

By consider $V_g = 0$, then $[V_{abc}] = [P_{abc}][Q_{abc}]$ (A1.19)

Where $[P_{abc}]=[P_A]-[P_B][P_D]^{-1}[P_C]$. The phase capacitance matrix of the transmission line is : $[C_{abc}]=[P_{abc}]^{-1}$. (A1.20)

The capacitance matrix is in nodal form, which means that the diagonal element of C_{ti} is the sum of the shunt capacitances per unit length connected to conductor i; and the off-diagonal element $C_{ij}=C_{ji}$ is the negative shunt capacitance per unit length between conductor i and j. The element of capacitance matrix is as follows :

$$[C_{abc}]=\begin{bmatrix} C_{aa} & -C_{ab} & -C_{ac} \\ -C_{ab} & C_{bb} & -C_{bc} \\ -C_{ac} & -C_{bc} & C_{cc} \end{bmatrix} \qquad \text{(A1.21)}$$

The elements of shunt capacitance matrix usually are not balanced. A balanced condition can be obtained by full transposition of the line. The shunt capacitance matrix of a transposed line is as follows :

$$[C_{abc}]=\begin{bmatrix} C_s & -C_m & -C_m \\ -C_m & C_s & -C_m \\ -C_m & -C_m & C_s \end{bmatrix} \qquad \text{(A1.22)}$$

where :

$C_s = \frac{1}{3}(C_{aa}+C_{bb}+C_{cc})$ (A1.23a)

$C_m = \frac{1}{3}(C_{ab}+C_{ab}+C_{ac})$ (A1.23b)

The symmetrical component of the shunt capacitance is :

$$[C_{012}] = [T]^{-1}[C_{abc}][T] \qquad \text{(A1.24)}$$

For a transposed line, the symmetrical component capacitance is:

$$[C_{012}]=\begin{bmatrix} C_0 & 0 & 0 \\ 0 & C_1 & 0 \\ 0 & 0 & C_2 \end{bmatrix} \qquad \text{(A1.25)}$$

where

$$\begin{aligned} C_0 &= C_s - 2C_m \\ C_1 &= C_2 = C_s + C_m \end{aligned} \qquad \text{(A1.26)}$$

Inversely

$$\begin{aligned} C_m &= \tfrac{1}{3}(C_1 - C_0) \\ C_s &= \tfrac{1}{3}(C_0 + 2C_1) \end{aligned} \qquad \text{(A1.27)}$$

APPENDIX 2

VARIATION OF SECONDARY ARC DURATION WITH SECONDARY ARC CURRENT AND RECOVERY VOLTAGE

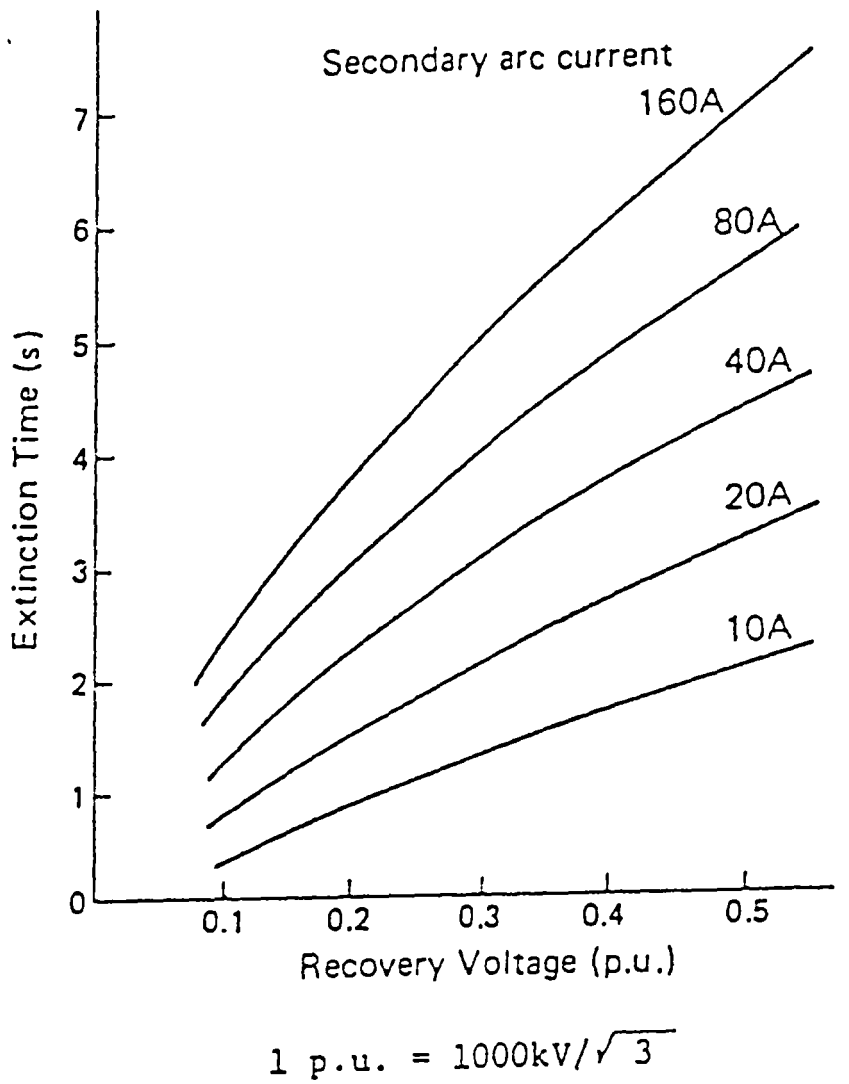

Figure-A2.1: The Variation of secondary arc duration with secondary arc current and recovery voltage for a 1000 kV transmission line [21].

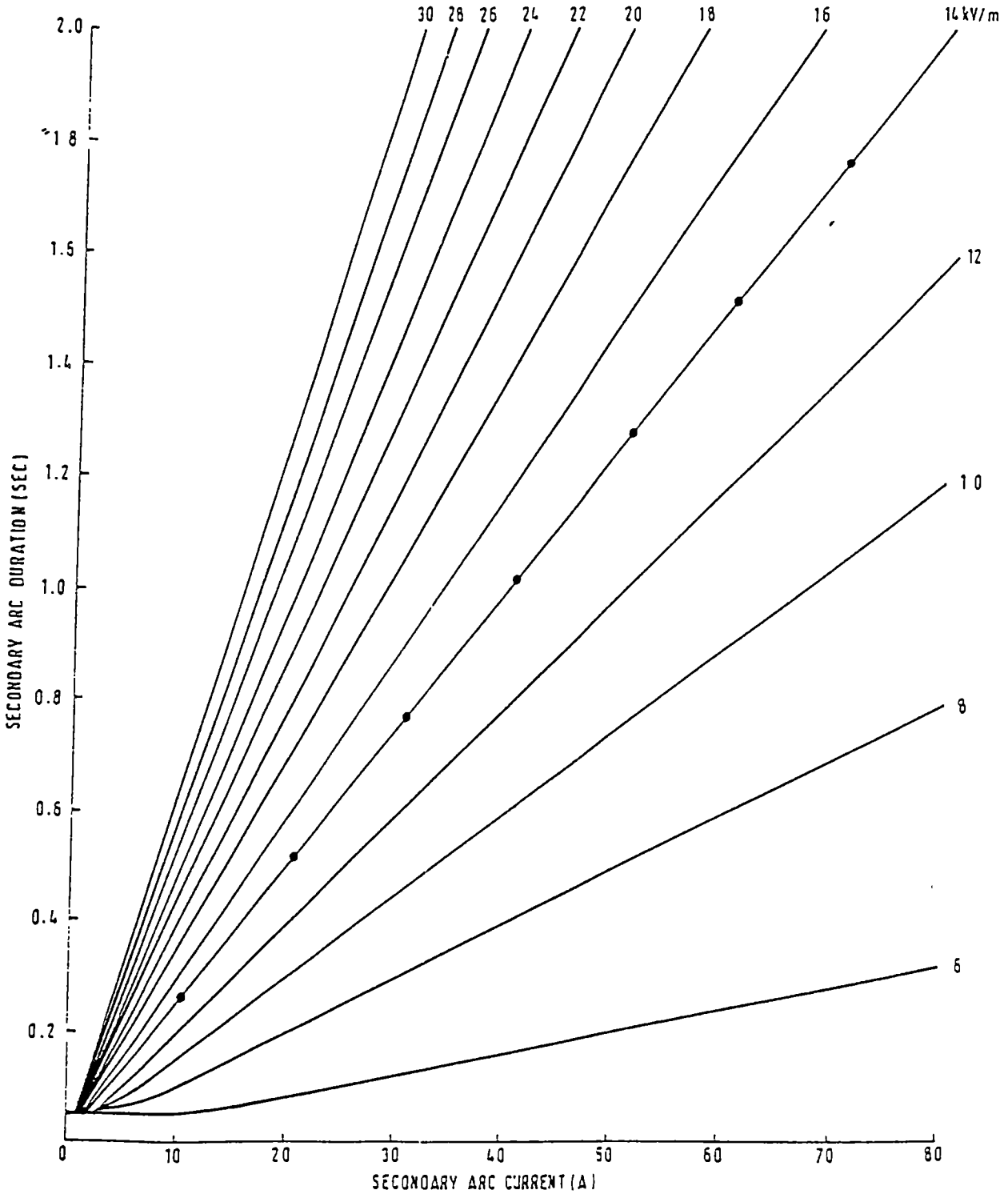

Figure-A2.2: The Variation of secondary arc duration with secondary arc current and gradient recovery voltage for transmission lines up to 700 kV [8,17].

APPENDIX 3

SIMULATION VERIFICATION

All studies involving transient simulation need to be verified using well established engineering methods in order to exclude possibility of making major error in modelling, model data or modelling assumptions. This appendix provides an example of hand calculations used to verify the simulated values of the secondary arc current and the recovery voltage for the 500 kV unloaded, transposed transmission line.

The line parameters used for the following calculations were obtained from the output of EMTP software. Even though both programs, EMTP and EMTDC, applied the same theoretical background for electromagnetic transient calculation, they produce different output format, especially for the transmission line parameter output. Both programs use the E.Clarke mode transformation instead of the symmetrical component, to ignore the complex number calculation [2,16]. The EMTP output produces transmission line parameters in symmetrical component format which is useful for hand calculations, while the output of EMTDC T-line program is in the modal form.

Based on the EMTP output, for transposed line:

For 4xGannet conductor, $B_0' = 2.45x10^{-06}$ mho/km, $B_1' = 3.85x10^{-06}$ mho/km.
For 4xDove conductor, $B_0' = 2.44x10^{-06}$ mho/km, $B_1' = 3.83x10^{-06}$ mho/km.
The line segment of Bandung-Ungaran consists of 120 km Dove conductor and 224 km Gannet conductor. Therefore, the total zero and positive capacitive susceptance of the line segment are: $B_0' = 840.56x10^{-06}$ mho, and $B_1' = 1319.92x10^{-06}$ mho.

Steady State Secondary Arc Current

The steady state arc current was calculated at no load condition and without reactor compensation. The secondary arc current at this condition is mainly caused by the mutual capacitive coupling, equation (3.5).

$$I_{sc} = -\frac{V}{3} j(B_1' - B_0')$$

$$I_{sc} = \frac{288.7}{3}(1319.92 - 840.56)$$

$$I_{sc} = 46.13A$$

Steady State Recovery Voltage

$$V_r = V\frac{(C_1 - C_0)}{(C_0 + 2C_1)}$$

$$V_r = 288.7\frac{(1319.92 - 840.56)}{(840.56 + 2639.84)}$$

$$V_r = 39.97kV$$

Four-legged Reactor Design

Assuming compensation factor F=60% then,

$$B_1 = FB_1' = 0.6x1319.92x10^{-06}mho = 791.95x10^{-06}mho$$

The reactor phase reactance is

$$X_p = \frac{1}{B_1} = \frac{1}{791.95x10^{-06}} = 1262\,Ohm$$

To calculate the reactor neutral reactance, first the line neutral susceptance (capacitive) is calculated below :

$$B_n' = \frac{3B_0'B_1'}{B_1' - B_0'} = \frac{3x1319.92x840.56x10^{-12}}{(1319.92 - 840.56)x10^{-6}} = 6943.5x10^{-06}\,mho$$

The reactor neutral reactance is:

$$X_n = \frac{1}{F B_n' \left[1-(1-F)\frac{B_1'}{B_0'}\right]} = \frac{1}{0.6(69435)x\left[1-(1-0.6)x\left(\frac{131992}{840.56}\right)\right]x10^{-06}}$$

$$X_n = 645\ Ohm$$